Molecular Biology and Evolution
Status: in review
Submitted: 17 - February - 2017
Article: Discoveries

Molecular evidence for the early evolution of photosynthetic water oxidation

Tanai Cardona[1*], Patricia Sánchez-Baracaldo[2], A. William Rutherford[1], Anthony Larkum[3]

[1]Department of Life Sciences, Imperial College London, London, UK
[2]School of Geographical Sciences, University of Bristol, Bristol, UK
[3]University of Technology Sydney, Ultimo NSW, Australia
*Correspondence to: t.cardona@imperial.ac.uk

Abstract

The evolution of Photosystem II changed the history of life by oxygenating the Earth's atmosphere. However, there is currently no consensus on when and how oxygenic photosynthesis originated. Here we present a new perspective on the evolution of oxygenic photosynthesis by studying the evolution of D1 and D2, the core subunits of Photosystem II, as a function of time. A Bayesian relaxed molecular clock approach was applied to the phylogeny of Type II reaction center proteins using geochemical constraints and calibrations derived from the fossil record of Cyanobacteria and photosynthetic eukaryotes. The resulting age estimates were interpreted in the context of the structure and function of photochemical reaction centers. Firstly, we point out it is likely that the ancestral protein to D1 and D2 gave rise to a photosystem that was capable of water oxidation. Secondly, our results indicate that the gene duplication event that led to the divergence of D1 and D2 is likely to have occurred more than a billion years before the emergence of the last common ancestor of extant Cyanobacteria. Thirdly, we show that it is unlikely that Cyanobacteria obtained photosynthesis via horizontal gene transfer. Furthermore, the data strongly suggest that the origin of photosynthesis in the early Archaean was necessarily followed by a rapid diversification of reaction center proteins, which included the divergence of D1 and D2. It is therefore concluded that primordial forms of water oxidation could have originated relatively soon after the emergence of photosynthesis.

Introduction

Geochemical evidence for photosynthesis

Anoxygenic photosynthesis was well stablished by 3.5 Ga. This is demonstrated by both sedimentological and isotopic evidence for photoautotrophic microbial communities recorded in Paleoarchean rocks (Tice and Lowe 2004; Nisbet and Fowler 2014; Butterfield 2015). In addition, sedimentary rocks and banded iron formations from Isua, Greenland, hint at the presence of photosynthetic bacteria in the marine photic zone as early as 3.7-3.8 Ga (Schidlowski 1988; Rosing 1999; Rosing and Frei 2004; Grassineau, et al. 2006; Czaja, et al. 2013; Knoll 2015). There is consensus that during most of the Archean, the world was largely anaerobic with oxygen concentrations staying below 10^{-5} of present atmospheric levels (Lyons, et al. 2014). Only about 2.4 Ga did atmospheric oxygen concentrations increase by several orders of magnitude (Bekker, et al. 2004) to about 10^{-2} to 10^{-1} of current levels; this point in time is known as the Great Oxidation Event (GOE) and sets a firm constraint on the minimum age for the evolution of oxygenic photosynthesis (Lyons, et al. 2014; Fischer, et al. 2016). However, the origin of oxygenic photosynthesis still remains controversial. There is much evidence for local oxygen 'oases' in the late Archean record, possibly going back to 3.0 Ga (Riding, et al. 2014), but it has been reported that oxygen was present in sedimentary deposits as old as 3.7 Ga based on redox-sensitive trace elements (Rosing and Frei 2004; Lyons, et al. 2014; Planavsky, et al. 2014; Satkoski, et al. 2015; Frei, et al. 2016). While there is some consensus from geochemical evidence that anoxygenic photosynthesis originated in the early Archaean, there is much greater uncertainty for the origin of oxygenic photosynthesis. It is clear however that the emergence of photosynthesis before 3.5 Ga means that the origin of photochemical reaction centers must predate this date.

Molecular evolution of Type II reaction centers

Here we wish to highlight several aspects of the evolution of anoxygenic and oxygenic photosynthesis that can be elucidated from a careful inspection of the phylogeny of the reaction center proteins, when considered in a structural context. Chief among these aspects is that the transition from anoxygenic to oxygenic photosynthesis must have initiated when an ancestral Type II reaction center evolved the capacity to oxidize water to oxygen (Michel and Deisenhofer 1988; Rutherford 1989). Today, water oxidation is catalyzed by the Mn_4CaO_5 cluster of Photosystem II (PSII) of Cyanobacteria and photosynthetic eukaryotes. Therefore, a complete scenario for the origin of oxygenic photosynthesis must explain how and when Type II reaction centers diversified and how and when one of these reaction centers evolved the Mn_4CaO_5 cluster. The evolution of Type II reaction center proteins has been described and discussed in some detail before (Beanland 1990; Nitschke and Rutherford 1991; Blankenship 1992; Rutherford and Nitschke 1996; Sadekar, et al. 2006; Cardona 2015, 2016) and it is schematized in fig. 1A.

Figure 1A illustrates that the core subunits of PSII, D1 and D2, and the core subunits of the anoxygenic Type II reaction centers, L and M, share a common origin (Beanland 1990). That is to say that D1, D2, L and M, all descended from a single protein. This ancestral protein is denominated **II** in fig. 1A. However, D1 and D2 share between each other significantly more sequence identity than either of them share with L or M, and this is reflected in greater structural identity between D1 and D2. The same is true the other way around, L and M share between each other significantly more sequence identity than either of them does with D1 or D2, and this is accordingly translated into greater structural similarity between L and M (Fig. 1). Thus, the ancestral core protein **II** diversified into two forms, one ancestral to D1 and D2, and the other ancestral to L and M. The ancestral protein to D1 and D2 is denominated **D0** in fig. 1. The ancestral protein to L and M is denominated **K**. Hence, D1 and D2 originated from a gene duplication event and makes a monophyletic clade of Type II reaction center proteins, distinct from that which gave rise to L and M.

It is worth noting that the monophyletic relationship of D1 and D2 implies that PSII core proteins cannot be derived from L and M proteins, and thus Cyanobacteria could not have obtained Type II reaction center proteins from Proteobacteria or Chloroflexi. From fig. 1A it is clear that the evolutionary event that led to the divergence of **D0** and **K**, marked **2**, predate the diversification event that led to the divergence of L and M, marked **4** and **5**. In other words, while D1 and D2 share common ancestry with L and M, the former did not originate from the latter, instead both families evolved in parallel. This was first noted by Beanland (1990) and it is corroborated by more detailed phylogenetic studies that integrate structural and functional comparisons of the reaction center proteins, see for example Sadekar, et al. (2006). A first corollary of the early divergence of **D0** and **K** is that the most ancestral Type II reaction centers were homodimeric: thus, a homodimeric reaction center made with subunit **K** was ancestral to the anoxygenic Type II reaction centers, and a homodimeric reaction center made of **D0** was ancestral to PSII. A second corollary is that the ancestral Type II reaction center, made of a homodimer of ancestral protein **II**, cannot be described as being more similar to L or M, than to D1 and D2. For this reason and rather counterintuitively, there is no phylogenetic evidence against the possibility that the most ancestral Type II reaction centers (**II**) were capable of water oxidation. Furthermore, a third corollary that has not yet been fully appreciated, but was recently pointed out by Cardona (2015), is that the divergence of D1 and D2 (**2**) is likely to have predated the evolution of Chloroflexi-type and Proteobacteria-type L and M proteins (**5**). However, this third corollary cannot be corroborated until a study of the rates of evolution of the distinct reaction center proteins is carried out.

Molecular evolution of Photosystem II core proteins

In order to talk precisely about the evolution of oxygenic photosynthesis at a particular point in time relative to the diversification of the domain, Bacteria, it is necessary to define the last common ancestor of Cyanobacteria. Here we define *the last common ancestor of Cyanobacteria* as the most

recent ancestor between the genus *Gloeobacter*, the earliest branch in the cyanobacterial tree of life, and all other extant strains; excluding the recently described non-photosynthetic Melainabacteria (Soo, et al. 2014). Under this definition, the last common ancestor of Cyanobacteria was already capable of efficient oxygenic photosynthesis because it had a PSII able to coordinate a Mn_4CaO_5 cluster virtually indistinguishable from that of extant Cyanobacteria (Cardona, et al. 2015). This is based on the observation that even the earliest diverging Cyanobacteria, the strains of the genus *Gloeobacter* (Honda, et al. 1999; Sanchez-Baracaldo, et al. 2005; Blank and Sanchez-Baracaldo 2010; Shih, et al. 2013), encode in their genomes a standard set of genes for the assembly of PSII (Nakamura, et al. 2003; Saw, et al. 2013) and can oxidize water by a mechanism identical to those of later evolving strains (Koyama, et al. 2008).

The Mn_4CaO_5 cluster of PSII is coordinated mainly by the D1 protein (Nixon and Diner 1994; Ferreira, et al. 2004), which provides seven ligands to the cluster (fig. 2). The structure of the cluster has been resolved in detail by Umena, et al. (2011) and Suga, et al. (2015). Among reaction center proteins D1 has the most complex evolutionary history, which was described in detail by Cardona, et al. (2015) and is schematized in fig. 1B. At least five different well-defined types of D1 have been identified. The early evolving forms, referred to as atypical D1 forms, are characterized by the absence of some of the ligands to the Mn_4CaO_5 cluster. There are three distinct groups of atypical forms: the earliest evolving D1 retained in the genome of *Gloeobacter kilaueensis* (G0 in fig. 2) (Cardona, et al. 2015), super-rogue D1 (Murray 2012) or chlorophyll *f* synthase (G1) (Ho, et al. 2016), and the rogue D1 (Murray 2012) or sentinel D1 (G2) (Wegener, et al. 2015). It is noteworthy that Ho, et al. (2016) proposed that chlorophyll *f* synthase is a homodimeric reaction center made of a pair of super-rogue D1, this would fit with the idea that early Type II reaction centers were indeed homodimeric.

The late evolving forms of D1, also referred to as the standard D1 forms, are characterized by having a complete ligand sphere for the Mn_4CaO_5 cluster and can be subdivided into two groups: the microaerobic form of D1 (G3) expressed under low oxygen concentrations (Sicora, et al. 2009) and the dominant form of D1 (G4), which is present in the genome of all Cyanobacteria and photosynthetic eukaryotes with PSII and it is the main form of D1 associated with water oxidation catalysis. Previous phylogenetic studies seemed to suggest that the microaerobic form (G3) branched out before the dominant form of D1 (G4) diversified (Cardona, et al. 2015). Remarkably, a water-splitting PSII with a microaerobic form of D1 is more efficient and robust than a PSII with a dominant form of D1 under low-oxygen concentrations (Crawford, et al. 2016). This observation may suggest that the dominant form of D1 evolved as a response to increasing oxygen concentrations within the cell and the environment (Cardona, et al. 2015).

Both the phylogeny of D1 proteins and the ancestral traits retained in the atypical D1 sequences suggest that these atypical forms might have branched out at different stages during the evolution of water oxidation but prior to the evolution of the standard forms of D1. In this way, it can

be deduced from the available sequence data that the Mn_4CaO_5 cluster reached its current configuration (Umena, et al. 2011), at least in the ancestral state of D1 before the divergence of the microaerobic (G3) and dominant forms (G4).

The phylogeny of D1 is also characterized by an extensive number of duplication events occurring at every taxonomic level (Cardona, et al. 2015), some of which are ancient and gave rise to the atypical forms, but many of which are much more recent. Therefore, every cyanobacterium with multiple *psbA* genes can carry several identical copies encoding identical D1 subunits, which are the result of recent gene duplications, and copies with different degrees of divergence, which are the result of more ancestral duplication events. The phylogeny of D1 also shows that every cyanobacterium with PSII has at least one *psbA* gene encoding a dominant form of D1 (G4). For example, *Gloeobacter kilaueensis* has a genome with six *psbA* genes, five encode dominant forms (G4), three of these five have identical amino acid sequences, while the other two show some level of sequence divergence. The sixth gene encodes a unique atypical sequence, designated here G0. In contrast, *Gloeobacter violaceous* lacks the atypical sequence but has the other five D1 sequences. Another example is *Chroococcidiopsis thermalis*, which has in its genome six different *psbA* genes, four encoding different dominant forms of D1 (G4), in addition to a rogue D1 (G2) and a super-rogue D1 (G1) with chlorophyll *f* synthase activity (Ho, et al. 2016).

Altogether, the distribution and phylogeny of D1 proteins indicate that the last common ancestor of Cyanobacteria already carried in its genome a dominant form of D1 (G4), which implies that the gene duplication events that led to the origin of the microaerobic form of D1 (G3) and the atypical sequences (G0, G1, G2) predated this last common ancestor and the diversification of crown group Cyanobacteria (Cardona, et al. 2015). The phylogeny of D1 shows that the last common ancestor of Cyanobacteria existed at a very advanced stage in the evolution of oxygenic photosynthesis and PSII water oxidation. If so, how long did it take for an ancestral Type II reaction center to evolve into the sophisticated water-oxidizing photosystem inherited by Cyanobacteria and photosynthetic eukaryotes?

The ancestral photosystem prior to the divergence of D1 and D2

As a result of the monophyletic relation of D1 and D2 and the conserved structural and functional characteristics between these proteins, it is possible to reconstruct with confidence some of the traits of the ancestral photosystem. These conserved characteristics, present in both D1 and D2, but absent in L and M, strongly suggest that the ancestral homodimeric photosystem, made of a **D0** dimer, had most of the traits known to be associated with the highly oxidizing potential of standard PSII and required for water oxidation (Rutherford and Nitschke 1996; Rutherford and Faller 2003; Cardona, et al. 2012; Cardona 2016).

Four structural domains differentiate D1 and D2 from L and M (fig. 2A). These are: 1) the N-terminus, which is essential for the efficient disassembly and repair of these subunits upon

photodamage, which occurs by a mechanism that is identical for D1 and D2 (Komenda, et al. 2007; Krynicka, et al. 2015). 2) A segment between the 1st and 2nd transmembrane helices, which is required for protein-protein interactions with the small subunits and the extrinsic polypeptides (Cardona 2015, 2016). The small subunits are required for assembly and stability of the complex and none of them is present in anoxygenic reaction centers (Dobakova, et al. 2007; Komenda, et al. 2012; Sugiura, et al. 2015). The extrinsic polypetides are important for the stability of the cluster, in particular PsbO (Franzen, et al. 1985; De Las Rivas, et al. 2004; Roose, et al. 2016). 3) An extended loop between the 4th and the 5th transmembrane helices required for the coordination of bicarbonate, which is important for regulation and photoprotection (Ferreira, et al. 2004; Brinkert, et al. 2016). 4) An extended C-terminus necessary for the coordination of the Mn_4CaO_5 cluster, Cl^- binding, water channels, and proton pathways (Debus 2001; Umena, et al. 2011; Linke and Ho 2013). All four of these structural differences are either directly required for water oxidation or are necessary for stability of the complex, assembly, repair, and photoprotection. The strong inference that can be made from these structural characteristics is that before the divergence of D1 and D2, the ancestral photosystem was already undergoing evolutionary changes to support water oxidizing chemistry and to deal with radical oxygen species.

Further evidence for water oxidation prior to the divergence of D1 and D2 can be observed at the sequence and cofactor level. A redox tyrosine-histidine pair is conserved in both D1 and D2, this demostrates that the $P/P^{+\bullet}$ chlorophyll redox pair in this ancestral photosystem was able to generate enough oxidizing power to form a neutral tyrosyl radical on either side of the homodimeric reaction center (Rutherford and Nitschke 1996; Rutherford and Faller 2003). In addition, several potential metal ligands are traceable to **D0**, at least two glutamate at positions equivalent to 170 and 189 of standard D1, a histidine at position equivalent to 337, and an additional ligand to the Mn_4CaO_5 cluster is provided from the ancestral protein of the CP43 and the CP47 subunits (Cardona, et al. 2015; Cardona 2016), fig. 2B. Conserved carotenoids near the peripheral reaction center chlorophylls, Chl_Z and Chl_D, implies the presence of photoprotective mechanism to quench triplet chlorophyll states and the existence of electron transfer side pathways (Krieger-Liszkay, et al. 2008; Cardona, et al. 2012), which are in place to prevent the formation of singlet oxygen. Conserved tyrosine residues on both D1 (Y246) and D2 (Y244), which provide hydrogen bonds to the bicarbonate ligand of the non-heme iron (Umena, et al. 2011), suggest that this was present in the ancestral homodimeric photosystem, made of **D0,** fig. 2C. The binding of bicarbonate has now been shown to modulate the potential of the quinones as a protective mechanism against singlet oxygen formation (Brinkert, et al. 2016). It can be concluded that the ancestral photosystem made of **D0** was able to oxidize water accompanied by the unavoidable production of radical oxygen species, which then required the innovation of protective measures. It is plausible that the ancestral photosystem oxidized manganese and coordinated a primordial catalytic cluster. From this it follows that the heterodimerization process of D1 and D2, culminating with the appearance of the standard form of D1, was consequently a path to optimization

of: 1) water oxidation efficiency (Rutherford, et al. 2012), 2) photoprotective mechanisms against radical oxygen species (Krieger-Liszkay, et al. 2008), and 3) photoactivation of the Mn_4CaO_5 cluster, assembly, and repair of the protein complex in the presence of oxygen (Nixon, et al. 2010; Nickelsen and Rengstl 2013).

Reformulating the evolution of oxygenic photosynthesis

Prior to the evolution of the standard form of D1 several stages in the evolution of oxygenic photosynthesis can be envisaged: the earliest of these stages is the divergence of Type I and Type II reaction center proteins (**1**, fig. 1A); this is then followed by the divergence of the *anoxygenic* family (L/M) and *oxygenic* family (D1/D2) of Type II reaction center proteins (**2**), then by the duplication event that led to the divergence of D1 and D2 (**3**), and the subsequent (**7**) gene duplication events and specializations that created the known diversity of D1 forms, which ultimately resulted in the emergence of the dominant form of D1 (G4) that characterizes PSII. If **D0** was able to support water oxidation chemistry, then the earliest stages in the evolution of oxygenic photosynthesis occurred between stages **2** and **3** as depicted in fig. 1A.

The evolution of oxygenic photosynthesis can be conceptualized from the molecular phylogeny of Type II reaction centers as the span of time between **D0** and the ancestral standard form of D1 (marked **8** in fig. 1B). This span of time, or the difference in time between the earliest possible occurrence of water oxidation recorded in the molecular record and the appearance of the standard form of D1, representing modern-day PSII, we denote by **ΔT**. If **ΔT** is small, a few million years or less for example, it could be concluded that the evolution of oxygenic photosynthesis was a sudden and fast process. This scenario would imply that oxygenic photosynthesis evolved rapidly just before the GOE as suggested recently by Ward, et al. (2016) or Shih, et al. (2017). On the other hand, if **ΔT** is large, several hundred million years or more for example, it would be consistent with oxygenic photosynthesis emerging long before the GOE as suggested by some geochemical (Planavsky, et al. 2014; Satkoski, et al. 2015) and phylogenetic data (Blank and Sanchez-Baracaldo 2010; Schirrmeister, et al. 2013; Schirrmeister, et al. 2015).

Here we applied Bayesian relaxed molecular clock analyses to assess the magnitude of **ΔT** and the dynamics of the rates of evolution of Type II reaction center proteins. We maximize the number of calibrations and constrict the clock with geochemical constraints and previously implemented fossil constraints across Cyanobacteria and photosynthetic eukaryotes from the Proterozoic and Phanerozoic. The data presented here indicate that the evolution of oxygenic photosynthesis is more likely to have been a long and gradual process starting early during the evolutionary history of life.

Results

Change in sequence identity as a function of time

A first approximation to the evolution of Type II reaction centers as a function of time can be derived from the level of sequence identity between D1 and D2 of different species with known divergence times as shown in fig. 3. For example, the D1 protein of the dicotyledon *Arabidopsis thaliana* shares 99.7% amino acid sequence identity with that of the dicotyledon *Populus trichocarpa*, which are estimated to have diverged between 127.2 and 82.8 Ma (Clarke, et al. 2011), fig. 3 and supplementary table S1. On the other hand, *A. thaliana*'s D1 shares 87.7% sequence identity with that of the red alga *Cyanidioschyzon merolae*. Red algae are known to have diverged at least 1.2 Ga ago (Butterfield 2000). At the other end of this evolutionary line, the three dominant forms of D1 from *Gloeobacter violaceous* share on average 79.2% sequence identity with that of *C. merolae* or 78.5% with that of *A. thaliana*. If the percentage of sequence identity between pairs of species is plotted as a function of their divergence time, a linear decrease of identity is observed among reaction center proteins at a rate of less than 1% per 100 million years (supplementary table S2).

It should be noted that uncertainties in the fossil record of photosynthetic eukaryotes would result in only small changes to this trend, as this is strongly constrained by the presence of the dominant forms of D1 and D2 in all extant Cyanobacteria. If the last common ancestor of Cyanobacteria existed hundreds of millions of years before the GOE, this would presuppose an even slower rate of evolution of the core subunits of PSII. On the other hand, if the rate of evolution of D1 and D2 are taken at face value, following the roughly uniform rate observed in photosynthetic eukaryotes, this would locate the divergence of *Gloeobacter* after the GOE (fig. 3, red spot).

All reaction center proteins originated from a single ancestral protein that diversified as the multiple groups of photosynthetic bacteria arose. As a result of this common ancestry, any standard D1 shares on average 30% sequence identity with any D2 across their entire sequence. Any standard D1 or D2 share on average 17% sequence identity with any L or M. The level of sequence identity falls well below 5% if any Type II reaction center protein is compared with any Type I reaction center protein (Cardona 2015). In consequence, the rate of evolution of D1 and D2 since the GOE, as estimated from the decrease of sequence identity (<1% per 0.1 Ga), is too slow to account for the evolution of photochemical reaction centers under any circumstances (fig. 3, dashed line). In other words, any scenario for the origin of photochemical reaction centers in the Archaean requires initially faster rates of evolution than in the later stages.

Bayesian relaxed molecular clock analysis

While the simple approach used above indicates that the divergence of D1 and D2 must be placed well before 3.0 Ga, it is possible to make further inferences on the evolution of oxygenic photosynthesis by applying a relaxed molecular clock approach to the phylogeny of Type II reaction center proteins and from the resulting rates of evolution. Fig. 4 shows a Bayesian relaxed log-normal autocorrelated molecular clock built using the CAT + GTR + Γ model allowing for flexible boundaries on the calibration points (Lartillot, et al. 2009). We specified the age of the root (root

prior) at 3.5 Ga with a standard deviation of 0.05 Ga. Under these conditions, the last common ancestral protein to the standard form of D1 prior to the divergence of the G3 and G4 types (fig. 4, green dot) is timed at 2.19 ± 0.22 Ga. On the other hand, **D0** (fig. 4, orange dot) is timed at 3.22 ± 0.19 Ga. It follows then that the difference in time between **D0** and the first standard form of D1, **ΔT**, is 1.02 Ga.

Table 1 shows estimates of divergence times of key ancestral Type II reaction center proteins and the respective **ΔT** value using different root priors. It can be seen, for example, that under the assumption that Type I and Type II reaction center proteins had already diverged 3.8 Ga ago, **ΔT** is found to be 1.17 Ga. Similarly, if the origin of photosynthesis is assumed to be a late event centered at 3.2 Ga, though unlikely, **ΔT** is still 0.90 Ga. These patterns show that regardless of the exact timing of the origin of photosynthesis, the evolution of oxygenic photosynthesis is extremely unlikely to have been a sudden event occurring in a few million years prior to the GOE.

Relaxing the boundaries on the calibration points by increasing the standard deviation on the root prior pushes the timing of the earliest events in the evolution of Type II reaction center to even older ages rather than younger ages (supplementary table S3). For example, a root prior of 3.5 Ga with a standard deviation of 0.1 Ga pushes the estimated time for the root to 3.65 Ga; and with a standard deviation of 0.2 Ga to 4.00 Ga. In the former case, **ΔT** shifts to 1.16 Ga and in the latter to 1.31 Ga.

Figure 4 additionally indicates that the divergence of the L and M subunits occurred *after* the divergence of D1 and D2. The estimated time for the divergence of L and M is centered at 2.87 ± 0.16 Ga, while the time for the divergence of D1 and D2, as we saw above, is 3.22 ± 0.19 Ga. The late divergence of L and M suggests that the divergence of D1 and D2 predates significantly the diversification event that led to the evolution of Chloroflexi-type and Proteobacteria-type L and M subunits, in agreement with the prediction by Cardona (2015).

The Bayesian analysis using flexible boundaries on the calibration points consistently produced ages for the divergence of the D2 subunit of *G. violaceous* and the dominant form of D1 (G4) after the GOE, in agreement with the work by Shih, et al. (2017). Yet, previous molecular clocks have suggested that the last common ancestor of Cyanobacteria might predate the GOE (Schirrmeister, et al. 2015), so we also performed a similar analysis that allowed us to explore this scenario. This was only achieved by the application of less flexible boundaries under an empirical amino acid substitution model (LG + Γ). We found this to be the only way to locate the D2 of *G. violaceous* and the dominant form of D1 (G4) before the GOE. The effect of less flexible boundaries on the estimated divergence times is shown in table 1. Assuming a root prior of 3.5 ± 0.05 Ga, the estimated divergence time for the standard form of D1 becomes 2.64 ± 0.15 Ga and pushes **D0** back to 3.40 ± 0.09 Ga, making **ΔT** 0.77 Ga. On the other hand, if we allowed flexibility on the root prior by increasing the standard deviation to 0.4 Ga (supplementary table S3), the estimated divergence time for the standard form of D1 becomes 2.83 ± 0.21, but the estimated age of the root is pushed

back to 3.92 ± 0.21 Ga with **D0** at 3.79 ± 0.21, making **ΔT** 0.96 Ga. Overall, placing the last common ancestor of Cyanobacteria before the GOE pushes the gene duplication event that led to the divergence of D1 and D2 even closer to the origin of Type II reaction centers.

Rates of evolution

Figure 3 suggests that the rates of evolution had to be faster at the initial stages than in the Proterozoic, even when **ΔT** is as large as 1.0 Ga. To have a better understanding of the changes of the rate of evolution of Type II reaction center proteine we plotted the rates as a function of divergence time. The rates are generated from the molecular clock analysis as described in Lepage, et al. (2007) and references therein.

Figure 5A plots the rate of evolution (**v**) of each node in the tree, expressed as amino acid substitutions per site per unit of time, against the estimated divergence time for each respective node. It can be clearly seen that the rate at the earliest stage is much faster than the rates observed since the Proterozoic. What is remarkable is that this is true even if the origin of Type II reaction centers is assumed to be 4.2 Ga, as seen in fig. 5B. The decrease in the rate of evolution is consistent with the observations derived from fig. 3 and appears to approximate a first-order exponential decay curve (supplementary table S4). Fig. 5A additionally shows that L and M have been evolving at a slightly faster rate than D1 and D2. From this slow-down of the rates of evolution it can be calculated that since each respective duplication event (**2** and **4** in fig. 1) it took about 168 million years for D1 and D2 to fall to 50% sequence identity and about 115 million years for L and M.

The maximum rate of evolution in the D1 and D2 family of reaction center proteins is placed at the node that represents D0. We will refer to this rate as $\mathbf{v_{max}}$. Fig. 5A shows that the rate of evolution flattens out at comparatively slow rates during the Proterozoic. These rates correspond to the rates of Group 4 D1 and D2. We will refer to the average rate of evolution during this zone of slow change as $\mathbf{v_{min}}$. The average rate $\mathbf{v_{min}}$ is thus defined as the average rate from each node in Group 4 D1 and D2. In fig. 5A, $\mathbf{v_{max}}$ is 5.03 amino acid substitutions per site per Ga, while $\mathbf{v_{min}}$ is 0.12 substitutions per site per Ga. Under the assumption that reaction centers had evolved by 3.5 Ga, these rates indicate that to account for the divergence of D1 and D2 in one billion years (**ΔT**), the initial rate of evolution had to be about 40 times larger than that observed since the last common ancestor of Cyanobacteria. For a comparison of rates of evolution of diverse proteins see table 2.

A fast rate of evolution at the earliest stage implies that $\mathbf{v_{max}}$ must increase if **ΔT** is smaller, as shown in Fig. 5B and 5C. The decrease in **ΔT** can only be obtained computationally by making the root prior younger, which correspondingly forces all nodes to younger ages. The increase of $\mathbf{v_{max}}$ with decreasing **ΔT** obeys a power law-function (supplementary table S5). For example, if **ΔT** is twenty times smaller; that is, if the divergence of D1 and D2 occurred in only 50 Ma, then $\mathbf{v_{max}}$ had to be many times larger, in this case 483.83 times larger than $\mathbf{v_{min}}$ as calculated by extrapolating from fig. 5C. In simple terms, if D1 and D2 diverged in 50 Ma the initial rate of evolution had to be 2443

amino acid changes per site per Ga, which would be comparable to the rate of evolution of some viruses, see table 2. Taking into consideration that reaction center proteins and many other proteins of importance in bioenergetics have changed little for billions of years, some as old as the last universal common ancestor (Weiss, et al. 2016), a virus-like rate of evolution seems quite improbable. Therefore, it is quite unlikely that the divergence of the core proteins of PSII was a sudden or very rapid event.

Sensitivity analysis

To test the robustness of the method we explored a range of contrasting models. We compared the effect of the model of relative exchange rates on the estimated divergence times. Fig. 6A plots estimated divergence times calculated with the CAT + GTR model (Yang and Rannala 2006) against divergence times calculated using the CAT model with a uniform (Poisson) model of equilibrium frequencies. Fig. 6A shows that the GTR model does not have a strong effect on the calculated divergence times as the slope of the graphs does not deviate from unity when paired with the uniform model (supplementary fig. S1 and table S6). Thus under a root prior of 3.5 ± 0.05 Ga a CAT + Poisson model also generated a **ΔT** of 1.02 Ga, see table 4.

To understand the effects of the oldest calibration point (point 11, fig. 4) on the estimated divergence time, we tested a second set of boundaries restricting this point to a minimum age of 2.7 Ga (Calibration 2) under the assumption that the divergence of the genus *Gloeobacter* may significantly predate the GOE. Fig. 6B shows a comparison of the two calibration choices on the overall estimated times for a flexible and a non-flexible model. If the divergence times using both calibrations are plotted against each other, a linear relationship is obtained (see supplementary fig. S2 and table S7). Calibration 2 did not seem to have a very strong effect on the estimated divergence times nor **ΔT**. For example, under a root prior of 3.5 ± 0.05 Ga and employing Calibration 2, **ΔT** was 0.97 Ga, see table 4.

In contrast, the choice of model for the evolution of substitution rates had a strong impact on the estimated divergence times (supplementary fig. S3 and table S8). Fig. 6C shows divergence time estimates of a tree calculated using a relaxed log-normal autocorrelated molecular clock plotted against a tree calculated using an uncorrelated gamma model on the rates of evolution. The autocorrelated model assumes that close branches are more likely to evolve at a similar rate, while the uncorrelated model assumes that the rate of evolution of each branch can vary independently (Lepage, et al. 2007; Ho and Duchene 2014). Under the uncorrelated model the estimated divergence times of many nodes were aberrantly shifted to younger ages: for example, most cyanobacterial and eukaryotic D1 clustered in the range of 700 to 0 Ma, which is inconsistent with the fossil record, and results in **ΔT** values of about 2.0 Ga. The molecular reason behind this difference may be related to the fact that photochemistry imposes strong constrains on the evolution of reaction center proteins. As all of them must coordinate and maintain all redox cofactors, chlorophylls, quinones, carotenoids, and a non-

heme iron, at a precise orientation and distance from each other to allow for control of electron transfer rates and redox potentials. These rates and potentials are crucial not only for function but also for protection against the formation of radical oxygen species (Cardona, et al. 2012; Rutherford, et al. 2012). It seems reasonable then, that the rates of evolution of all Type II reaction center proteins should be, to some extent, similar, and even more so among closely related groups, thus corresponding to an autocorrelated model.

Discussion

A complete scenario for the origin and evolution of oxygenic photosynthesis needs to account for the evolution of Type II reaction centers and in particular, D1 and D2, the core subunits of PSII. Our results indicate that the evolution of oxygenic photosynthesis cannot be described as a rapid event happening within a few million years before the GOE. Our results suggests that the evolution of oxygenic photosynthesis is better described as a long process, spanning nearly a billion years, and starting soon after the origin of the first photochemical reaction centers in ancestral populations of bacteria.

Change in sequence identity as a function of time

As an approximation to the evolution of the core subunits of PSII we plotted the level of sequence identity of D1 and D2 as a function of known divergence times (fig. 3). From this plot two main characteristics of the evolution of photosynthesis can be defined. Firstly, the three earliest stages in the evolution of photochemical reaction centers: 1) the divergence of Type I and Type II reaction centers, 2) the divergence of *anoxygenic* and *oxygenic* families of Type II reaction center proteins, and 3) the divergence of D1 and D2, were more likely to have occurred near the origin of photosynthesis rather than near the GOE. Taking into consideration that there is strong evidence for photosynthesis at 3.5 Ga, then these three stages could well predate this time. In addition, if photosynthesis is confirmed at 3.8 Ga, then the occurrence of these three events must, consequently, be pushed further back in time accordingly. Secondly, the last common ancestor of Cyanobacteria is more likely to have lived around the time of the GOE rather than shortly after the origin of photosynthesis. This common ancestor must have had a dominant form of D1 (G4), which places it relatively far after the origin of photosynthesis. The early divergence of D1 and D2 implies that the earliest stages in the evolution of oxygenic photosynthesis may predate the last common ancestor of Cyanobacteria by about 1.0 Ga.

Bayesian relaxed molecular clock analysis

The application of a molecular clock to the phylogeny of Type II reaction centers is strongly constrained by evidence of photosynthesis at 3.5 Ga, by the GOE at 2.45 Ga, and by the relatively slow rate of evolution of D1 and D2 for at least 2.0 Ga. These constraints could be in question if: 1) the geochemical evidence for photosynthesis in the early Archaean is the result of abiotic processed or

geological artifacts, 2) the GOE has an entirely abiotic cause, and 3) photosynthetic eukaryotes radiated at a much earlier time, in the Archaean instead of the Proterozoic. However, given the current state of knowledge these three opposing alternatives not only appear improbable, but also contradictory.

The application of those strong constraints listed above on the molecular phylogeny of Type II reaction centers revealed that the divergence of D1 and D2 must be a long process traceable to the earliest events in the history of photosynthesis, as sown in fig. 3. We highlight this long process by introducing the concept of **ΔT**, which defines two specific points in time in the evolution of D1 and D2. The magnitude of **ΔT** is dictated by the phylogenetic distance between D1 and D2 and their rate of evolution derived from the geochemical and fossil constrains. Therefore, it is not surprising that under most reasonable models employed in this analysis **ΔT** is always in the range of 1.0 Ga.

We have considered two possible evolutionary scenarios that are both consistent with a large **ΔT**. In the first scenario the standard forms of D1 start to diverge at about 2.4 Ga, as seen in fig. 4, and diversify into G3 and G4 after the GOE. If we consider that the last common ancestor of Cyanobacteria had a G4 D1, this would set it after the GOE. This scenario, derived from the application of a relaxed molecular clock using a non-parametric CAT model with flexible boundaries, is in agreement with the recent observations by Shih, et al. (2017) and other molecular clock studies that placed the divergence of *Gloeobacter* after the GOE (Feng, et al. 1997; David and Alm 2011; Marin, et al. 2017). In this scenario, under a root prior of 3.5 Ga, the divergence of D1 and D2 is set at about 3.2 Ga.

In the second scenario, we consider that the last common ancestor of Cyanobacteria occurs before the GOE as suggested by other molecular clock analyses (Falcon, et al. 2010; Sanchez-Baracaldo 2015; Schirrmeister, et al. 2015). In our work, this scenario is obtained with the application of a relaxed molecular clock using an empirical model (LG + Γ) with less flexible boundaries. In this scenario, under a root prior of 3.5 Ga, the appearance of the ancestral standard form of D1 is set at about 2.6 Ga. An age for a standard form of D1 of 2.6 Ga has the consequence of pushing the divergence of D1 and D2 closer to the root, and thus it is set at about 3.4 Ga (table 1). What can be concluded from this is that the older the last common ancestor of Cyanobacteria is, the more likely it is that the divergence of D1 and D2 occurred near the origin of photochemical reaction centers and thus, near the origin of photosynthesis.

In addition, the relaxation of the root prior constraints by increasing the standard deviation, invariably results in older estimated ages for the root (supplementary table S2). This result implies that it is more likely that photochemical reaction centers originated significantly before 3.5 Ga than after this time, which is consistent with the detection of ^{13}C-depleted organic carbon in 3.8 Ga rocks (Rosing 1999; Grassineau, et al. 2006) and by the existence of stromatolites of similar age (Nutman, et al. 2016), both from the Isua supracrustal belt in Greenland.

Horizontal gene transfer

There are two main competing hypotheses regarding the evolution of oxygenic photosynthesis in Cyanobacteria. One hypothesis states that Cyanobacteria obtained photosynthesis via horizontal gene transfer (HGT) from anoxygneic photosynthetic bacteria: see Raymond (2009) for a review and (Fischer, et al. 2016; Khadka, et al. 2017) for recent examples. This is designated here 'the HGT hypothesis'. The second hypothesis states that the evolution of two distinct reaction centers is a trait of the last common ancestor of all photosynthetic organisms and that the divergence of the two types of reaction centers initiated after an ancestral gene duplication event, see for example (Mulkidjanian, et al. 2006; Sousa, et al. 2013; Harel, et al. 2015). This is designated 'the duplication hypothesis'.

The HGT hypothesis implies that the two distinct reaction centers diverged in distinct phyla of bacteria and were transferred to an ancestral *non-photosynthetic* cyanobacterium before the evolution of water oxidation. The issue with this hypothesis is that it is inconsistent with the evidence for the molecular evolution of photochemical reaction centers, which shows that the core subunits of PSI and PSII branched out before the diversification of the anoxygenic reaction center proteins (Sadekar, et al. 2006; Cardona 2015). On the other hand, the duplication hypothesis leads to the question: "in which lineage did the gene duplication take place?" (Sousa, et al. 2013). Given that Cyanobacteria are the only bacteria with two reaction centers, this question often leads to the conclusion that photosynthesis originated in Cyanobacteria or a protocyanobacterium (Mulkidjanian, et al. 2006; Sousa, et al. 2013; Harel, et al. 2015). The issue with the duplication hypothesis is that it is in conflict with phylogenomic data, which consistently do not locate Cyanobacteria as a particularly early branching phylum in comparison with other phototrophic groups (Ciccarelli, et al. 2006; Wu, et al. 2009; Jun, et al. 2010; David and Alm 2011; Rinke, et al. 2013; Segata, et al. 2013; Marin, et al. 2017). Our results may provide enough detail to resolve this issue.

From fig. 4 it is concluded that the divergence event, marked **II**, predated the diversification events that led to the divergence of L and M, and also the divergence of this pair into Proteobacteria-type and Chloroflexi-type core proteins. Similarly, event **II** also predated the diversification events that led to the divergence of D1 and D2, and all the variety of D1 proteins found in Cyanobacteria. It follows then that event **II** had to have occurred before the diversification of the phyla Proteobacteria, Chloroflexi, and Cyanobacteria. Put another way, the phyla known to have Type II reaction centers had not yet diversified during the earliest events in the evolution of photosynthesis, when the ancestral reaction centers first diversified into Type I and Type II, and the subsequent gene duplications that resulted in the ancestral forms of L, M, D1, and D2. In agreement with these observations, an independent study performed by David and Alm (2011) identified a period of genetic innovation that coincided with a rapid diversification of the major bacterial lineages and the birth of a quarter of modern gene families. This period, between 3.33 Ga and 2.85 Ga, which the authors referred to as the Archaean Expansion, was suggested to be linked to the "bioavailability of oxygen", and was supported by the ancient origin of what the authors referred to as: "the basic genetic components

required for oxygenic photosynthesis and respiration". Our results put the divergence of D1 and D2 at 3.22 Ga and that of L and M at 2.87 Ga, which as we have seen, requires that the split between the *anoxygenic* and *oxygenic* branches of Type II reaction center proteins, event **II**, occurred by 3.5 Ga. It is worth noting that 3.5 Ga is likely to be a conservative estimate for the origin of photosynthesis. If photosynthesis is considerably older, say 3.8 Ga (Schidlowski 1988; Rosing 1999; Grassineau, et al. 2006; Czaja, et al. 2013; Knoll 2015), then this would imply an even older branching event for the ancestral core protein of PSII.

Taking into account that photosynthesis was well established by 3.5 Ga and that the major diversification of bacteria that resulted in the appearance of the described phyla is likely to have occurred later, in this so-called Archaean Expansion (David and Alm 2011), and as a consequence of the oxygenation of Earth and the evolution of eukaryotes (Battistuzzi and Hedges 2009; Brucker and Bordenstein 2012; Harel, et al. 2015; Marin, et al. 2017), it seems increasingly plausible that photosynthesis evolved near the root of the bacterial tree of life. The origin of photosynthesis was then rapidly followed by the divergence of the *anoxygenic* and *oxygenic* branches of reaction center proteins. The implication of this is that the earliest stages in the evolution of photosynthesis, including the appearance of the ancestral forms of D1 and D2, concomitant with water oxidation, is likely to have started prior to the divergence of most described groups of bacteria now known to bear photochemical reaction centers. Another implication of this early divergence is that the results provided by Mulkidjanian, et al. (2006), Sousa, et al. (2013), and Harel, et al. (2015) can be interpreted as evidence for two distinct reaction centers as a trait of ancestral populations of photosynthetic bacteria. A trait that today has been retained in Cyanobacteria and not acquired via horizontal gene transfer. From this perspective it can be concluded that this trait has been retained in Cyanobacteria since shortly after the origin of photosynthesis.

Recently, Shih, et al. (2017) reported a phylogenetic analysis of Cyanobacteria and their closest non-photosynthetic relatives, the Melainabacteria (Soo, et al. 2014). Shih, et al. (2017) postulated that Cyanobacteria acquired photosynthetic capacity via horizontal gene transfer after they diverged from the Melainabacteria. They hypothesized that the transfer of photosynthetic genes occurred from anoxygenic photosynthetic bacteria into a *non-photosynthetic* cyanobacterial ancestor with water oxidation evolving quickly before the GOE. Our results—which traced the evolution of the core subunits that allow the oxidation of water—show that not only is it unlikely that Cyanobacteria obtained photosynthesis via horizontal gene transfer, but it is also unlikely that the divergence of D1 and D2 from ancestral anoxygenic Type II reaction center proteins occurred rapidly just before the GOE. This leads to the conclusion that the origin of the Melainabacteria is more likely to have been initiated after ancestral losses of oxygenic photosynthesis.

The early evolution of photosynthesis as suggested by the geochemical record and the data we report here is consistent with photoautotrophy being an ancestral trait of early evolving bacteria and implies that the loss of it might be a derived trait in many phyla of bacteria. It is sometimes argued

that the loss of photosynthesis is unlikely due to the scattered distribution of reaction center proteins across the bacterial tree of life (Xiong, et al. 1998; Boucher, et al. 2003; Raymond 2009; Fischer, et al. 2016). Nevertheless, it has been shown repeatedly that gene loss is a very common process across all domains of life (Koskiniemi, et al. 2012; D'Souza, et al. 2014; Ku, et al. 2015; Albalat and Canestro 2016). For example, the majority of the proteins suggested to be in the universal ancestor by Weiss, et al. (2016) are not universally distributed, including those in carbon (e.g. Wood-Linjbal pathway), nitrogen (e.g. nitrogenase, glutamine synthase), and cofactor metabolism (e.g. siroheme, cobalamin), among many others, most of which are found to be scattered across the bacterial and archaeal domains. This fact implies ancestral and widespread gene loss across the entire tree of life. While horizontal gene transfer can only explain reacquisition of these processes after the universal ancestor, it cannot explain absence. Consistent with these observations, David and Alm (2011) showed that the period of rapid genetic innovation that peaked about 3.2 Ga is followed by a peak of massive gene loss a hundred million years later. It should not be at all surprising that clades of bacteria, which are specialized to live symbiotically and in aphotic environments (Di Rienzi, et al. 2013), or as predators (Soo, et al. 2015), such as the Melainabacteria, originated from ancestors that lost photosynthetic capacity. Several examples of the recent loss of oxygenic photosynthesis are the secondary loss of PSII by the symbiont *Atelocyanobacterium talassa* (Thompson, et al. 2012; Cornejo-Castillo, et al. 2016), the complete loss of photosynthesis of the cyanobacerium endosymbiont of *Epithemia turgida* (Nakayama, et al. 2014), and the case of parasitic Apicomplexa (Moore, et al. 2008) and holoparasitic angiosperms (Ravin, et al. 2016).

Ancestral losses of photosynthetic capacity do not imply that horizontal gene transfer of photochemical reaction centers has never occurred during the evolution of photosynthesis. Only a single unambiguous case of non-photosynthetic bacteria gaining phototrophy via horizontal gene transfer has been demonstrated so far; that is the case of *Gemmatimonas phototrophica* and closely related strains (Huang, et al. 2016), which obtained Type II reaction centers and bacteriochlorophyll synthesis from a gammaproteobacterium (Zeng, et al. 2014). All other suggested cases of ancestral horizontal gene transfer of photosynthesis in bacteria seem to be either very ancient, so that the direction of transfer is ambiguous—if it occurred at all—or between two photosynthetic strains. Examples of the latter case are the replacement of cyanobacterial rubisco for proteobacterial rubisco in red algae and dinoflagellates (Delwiche and Palmer 1996), the replacement of cyanobacterial protochlorophyllide reductase for the proteobacterial enzyme in marine *Synechococcus* and *Prochlorococcus* (Bryant, et al. 2012), and horizontal gene transfer of photosynthesis components between strains of Proteobacteria (Igarashi, et al. 2001) or between strains of Cyanobacteria (Sullivan, et al. 2006; Magnuson and Cardona 2016).

The most feasible case of *ancestral* horizontal gene transfer of Type II reaction centers supported by phylogenetic data might be between an ancestor of the Chloroflexi that predated the radiation event that led to the divergence of the Anaerolineae and Chloroflexia classes (Klatt, et al.

2011), and an ancestor of the Proteobacteria predating the radiation event that led to the Alpha-, Beta-, and Gammaproteobacteria classes (Swingley, et al. 2009; Tank, et al. 2009). However, at this stage there is not enough data available to directly infer the direction of the transfer.

Rates of evolution

If a strict molecular clock model were to be applied to the phylogeny of Type II reaction centers, the root of the tree would be placed long before the formation of the planet. Given the fact that the rate of evolution of D1 and D2 is restrained at comparatively slow rates from the Proterozoic until present times, the period of fast evolutionary change has to be located at the earliest stages to account for the evolution of photosynthesis within a reasonable timeframe. We found that even considering an age for the root of Type II reaction centers by 3.8 Ga the maximum rate during the evolution of D1 and D2, $\mathbf{v_{max}}$, is many times greater than the measured rates in the Proterozoic.

For the sake of argument, let us consider that an ancestral *non-photosynthetic* cyanobacterium obtained an anoxygenic Type II reaction center via horizontal gene transfer shortly after the divergence of Melainabacteria, 2.63 Ga ago, as suggested by Shih, et al. (2017). By 2.45 Ga this transferred anoxygenic Type II reaction center had evolved the capacity to oxidize water; that is 180 Ma after the Melainabacteria/Cyanobacteria split. It has been clear for some time that the source of the transferred anoxygenic Type II reaction center core proteins could not have been a member of the Proteobacteria or the Chloroflexi, as D1 and D2 are clearly not direct descendants of the L and M subunits found in these organisms. It becomes necessary to invoke the existence of a new lineage of undiscovered anoxygenic photosynthetic organisms that contained an anoxygenic reaction center made of D1- and D2-like proteins, at a point in time before the divergence of the atypical and standard forms of D1. A new question arises from these considerations, did the divergence of D1 and D2 occur before or after the horizontal gene transfer event? If it occurred after, that means that the divergence of D1 and D2 must have occurred in 180 Ma, which as we have seen is not supported by the rates of evolution, as this would require the existence of an exceedingly fast evolving reaction center that, all of a sudden, undergoes an extreme decline in the rate of amino acid changes. In this case, the rate of evolution upon transfer would be more than 800 times larger than the measured rates of evolution in the Proterozoic. On the other hand, in the even more unlikely case that the divergence of D1 and D2 occurred before the horizontal gene transfer, this would presuppose that D1 and D2 would have been diverging for a long period of time in this unknown lineage of bacteria. What is more, it would also presuppose that the capacity to oxidize water evolved before the horizontal gene transfer. In conclusion, a careful inspection of the evolution of reaction center proteins and their rates of evolution clearly indicates that the probability that an ancestral *non-photosynthetic* cyanobacterium obtained photosynthesis via horizontal gene transfer is negligible.

Another finding of the molecular clock analysis is that the divergence of L and M seems to occur after the divergence of D1 and D2. This is due to the slightly faster rates of evolution observed

for L and M at all periods of time. If we add to this the fact that L and M subunits are about 50 to 90 amino acids shorter than D1 and D2, it should take less time for L and M to converge into the ancestral node **K**. This raises the following question: if the heterodimerization of D1 and D2 was driven by optimization of water oxidation and the incorporation of photoprotective mechanisms, what selective pressures triggered the heterodimerization of L and M?

It has been proposed that the heterodimerization of Type II reaction centers was driven by the optimization of electron transfer efficiency and the avoidance of photodamage (Rutherford and Nitschke 1996; Rutherford and Faller 2003; Cardona, et al. 2012; Rutherford, et al. 2012). In a homodimeric Type II ancestor containing two identical exchangeable quinones, charge separation would result in enhanced back-reactions caused by electron transfer to a quinone site when empty or when occupied by a reduced form of the quinone (Rutherford and Nitschke 1996; Rutherford and Faller 2003); and additionally, by shorter back-reaction pathways (Cardona, et al. 2012; Rutherford, et al. 2012). Back-reactions from the early radical pairs give rise to chlorophyll triplet states in the heart of the reaction center (Dutton, et al. 1972; Rutherford, et al. 1981) and these triplet states are dangerous when they encounter oxygen, giving rise to the highly damaging singlet oxygen (Krieger-Liszkay, et al. 2008; Vass and Cser 2009; Rutherford, et al. 2012). In the oxygenic **D0** homodimeric ancestor of PSII, avoidance of photodamage could be a significant selective pressure for heterodimerization (Rutherford, et al. 2012). It seems clear that the enhanced back-reactions intrinsic to the homodimeric Type II reaction centers would have become a major problem whenever oxygen was present. The inefficient **D0** reaction center, as the primordial oxygenic photosystem, would have encountered this problem first and thus come under strong selection pressure toward heterodimerization at an early time. The results of the present work fit with this picture. Furthermore, our present finding that heterodimerization started significantly later in the anoxygenic homodimeric Type II reaction center (**K**) compared to its oxygenic counterpart (**D0**)**,** can be explained in this context as well, since **K** would have encountered these selection pressures much later, at a time when oxygen concentrations began to rise in localized environments in the late Archaean period, nearing the GOE (Bosak, et al. 2009; Lyons, et al. 2014; Riding, et al. 2014).

It is rather remarkable that anoxygenic Type II reaction centers contain an asymmetrically located carotenoid in contact with a core bacteriochlorophyll (Deisenhofer and Michel 1989). The role of this carotenoid is to quench bacteriochlorophyll triplet states in order to prevent the formation of singlet oxygen (Cogdell, et al. 2000). In addition, light-harvesting complexes in most anoxygenic photosynthetic bacteria contain carotenoids and perform a similar photoprotective function (Melo, et al. 2000; Kim, et al. 2007; Tsukatani, et al. 2012). As an extension of this, it does not seem unreasonable to think that even ancestral populations of anoxygenic phototrophic bacteria were under strong selective pressure by the threat of chlorophyll triplet-induced formation of radical oxygen species early during the evolutionary history of photosynthesis.

The phenomenon described here of an initial fast rate of evolution followed by an exponential decrease demands an explanation. Two possible mechanisms may account for this observation. The first one is the temperature dependent deamination of cytosine, as suggested by Lewis and coworkers (2016). They calculated that as the Earth cooled during its first 4 Ga, the rate of spontaneous mutation would have fallen exponentially by a factor of more than 4000. That is to say that the rate of spontaneous mutation during the earliest stages in the history of life would have been about three orders of magnitude greater than those observed since the Proterozoic. Lewis and coworkers (2016) calculated that 50% of all spontaneous mutations occurred in the first 0.2 Ga, which matches well with the exponential decay trend seen in fig. 5A, especially if an origin of photosynthesis is considered to be about 3.8 Ga. The second possibility is higher UV radiation on the planet's surface during the early Earth in the absence of an ozone layer, which could have resulted in rates of DNA damage up to three orders of magnitude greater than in present day Earth, as calculated by Cockell (2000); this higher rate of damage may have led as well to faster rates of change. Alternatively, both mechanisms could have contributed simultaneously.

Conclusion

This work demonstrates that the molecular evolution of photochemical reaction centers is consistent with an early Archaean origin of photosynthesis as inferred from geochemical evidence. We show that the origin of photosynthesis is likely to have been followed by a relatively rapid diversification leading to the divergence of *oxygenic* and *anoxygenic* families of reaction center proteins in ancestral populations of bacteria. In addition, our results support the premise that some form of water oxidation is highly likely to have evolved before the divergence of D1 and D2; because the ancestral protein to D1 and D2 branched out from the root of Type II reaction center proteins, it is plausible that primordial forms of biological water oxidation contributed to the deposition of the Isua banded iron formations (Rosing and Frei 2004; Frei, et al. 2016) and it is consistent with the persistent detection of oxygen hundreds of millions of years prior to the GOE (Lyons, et al. 2014). From the gene duplication event that permitted the divergence of D1 and D2, a billion years could have passed before the emergence of the standard form of D1 and the last common ancestor of crown group Cyanobacteria. Our results also show that the last common ancestor of Cyanobacteria existed at a relatively advanced stage in the evolution of oxygenic photosynthesis and yet it is likely that this ancestor descended from a lineage with an ancestry that can be traced, without obvious discontinuity, to the origin of the most primordial forms of photosynthesis. From this perspective, and taking into consideration the extensive diversity of D1 proteins, it is plausible that transitional forms of oxygenic photosynthesis existed with various degrees of complexity and efficiency at different stages following the origin of water oxidation catalysis in the ancestral homodimeric photosystem (Cardona, et al. 2015).

Materials and Methods

Type II reaction center proteins covering the known diversity of phototrophic bacteria were selected for this analysis. These include the L and M subunits from representatives of the phyla Proteobacteria, Gemmatimonadetes, and Chloroflexi and D1 and D2 proteins specific to the phylum Cyanobacteria and photosynthetic eukaryotes. A representative selection of D1 forms were obtained from Cardona, et al. (2015). These include the atypical D1 sequence found in the genome of *Gloeobacter kilaueensis* (Group 0), the super-rogue D1 or chlorophyll *f* synthase (Group 1), the rogue D1 or sentinel D1 (Group 2), the microaerobic D1 (Group 3), and the dominant form of D1 with sequences from both Cyanobacteria and photosynthetic eukaryotes (Group 4). In total 74 sequences were selected for the analysis, 30 D1, 20 D2, 10 L, and 14 M. Sequence alignments were performed using Clustal Omega employing ten combined guide trees and Hidden Markov Model iterations (Sievers, et al. 2011). To confirm that the alignment conformed with known structures, the 3D structures of the D1, D2, L and M, from the crystal structures 3WU2 (Umena, et al. 2011) of PSII and 2PRC (Lancaster and Michel 1997) of the anoxyenic Type II reaction center were overlapped using the CEalign (Jia, et al. 2004) plug-in for PyMOL (Molecular Graphics System, Version 1.5.0.4 Schrödinger, LLC) and structural homologous positions were cross-checked with the alignment. Maximum Likelihood phylogenetic analysis was performed using PhyML 3.1 (Guindon, et al. 2010) using the Blosum62 model of amino acid substitution. The amino acid equilibrium frequencies, proportion of invariable sites, and across site rate variation were allowed to be determined by the software from the dataset. Tree search operations were set as the best from the Nearest Neighbor Interchange and Subtree Pruning and Regrafting method, with the tree topology optimized using five random starts. The tree, which reproduced the phylogeny of Type II reaction center proteins, was then used as input for the Bayesian relaxed molecular clock analyses.

The phylogeny of Type II reaction centers was cross-calibrated on D1 and D2 as listed in table 4 and calibration points were allocated as presented in fig. 4, red dots. Dates for the *Arabidopsis*/*Populus* divergence, the appearance of the angiosperms, gymnosperms, and land plants were obtained from Clarke, et al. (2011). Dates for the divergence of Coscinodiscophyceae (Sims, et al. 2006), Floridiophyceae (Xiao, et al. 2004), and Rhodophyta (Butterfield 2000; Knoll, et al. 2013) were also included in the calibration. Furthermore, well-known cyanobacterial fossils were assigned to Nostocales (Golubic, et al. 1995; Schirrmeister, et al. 2016), Pleurocapsales (Golubic and Lee 1999; Sergeev, et al. 2002), and the first occurrence of multicellularity as represented by the early branching *Pseudanabeana* (Golubic and Lee 1999; Sergeev, et al. 2002; Schirrmeister, et al. 2016). The oldest calibration point, point 11, was selected to be the branching of the Group 4 D1 of *Gloeobacter violaceous* and was set to be around the age for the GOE with a minimum of 2.45 Ga and no maximum age (Calibration 1). In some cases, a calibration point 11 of 2.7 Ga was used for comparison (Calibration 2). The calibration points on D1 were allocated on Group 4 as this type of D1 is the only one retained in all Cyanobacteria with PSII and it is the only type of D1 inherited by

photosynthetic eukaryotes. The analysis by Cardona, et al. (2015) indicated that the gene duplication events that led to the atypical forms and the microaerobic forms of D1 are likely to predate the last common ancestor of Cyanobacteria. Therefore, it is the dominant form of D1 (G4) that more closely reproduced a species trees as the emergence of this type of D1 is roughly coincidental with the last common ancestor of Cyanobacteria, as described in Cardona, et al. (2015). The tree in fig. 4 was calculated using a root prior of 3.5 ± 0.05 Ga as a likely age for the evolution of photosynthesis. The evidence for photosynthesis in 3.5 Ga Archaean rocks has been reviewed extensively recently, see for example Nisbet and Fowler (2014), Butterfield (2015), or Knoll (2015). Nevertheless, we tested the effect of the root prior on the estimated divergence times as shown in table 1, by varying the root prior from 3.2 to 4.1 Ga and as shown in fig. 5B from 0.8 to 4.2 Ga.

A Bayesian Markov chain Monte Carlo approach was used to calculate the estimated divergence times using Phylobayes 3.3f , which allows for the application of a relaxed log-normal autocorrelated molecular clock under the CAT + GTR + Γ model (Lartillot and Philippe 2004; Lartillot, et al. 2009) necessary for the implementation of flexible boundaries on the calibration points (Yang and Rannala 2006). This model was compared with 1) a LG + Γ model that sets less flexible boundaries on the calibration points, 2) a CAT + Γ model assuming a uniform distribution of amino acid equilibrium frequencies (Poisson), or 3) an uncorrelated gamma model where the rates of substitution can vary independently. The flexible bounds were set to allow for 2.5% tail probability falling outside each calibration boundary or 5% in the case of a single minimum boundary. All molecular clocks were computed using four discrete categories for the gamma distribution and four chains were run in parallel until convergence.

In this work we define the period of time between the duplication event that led to the divergence of D1 and D2 and the appearance of the ancestral standard D1 as **ΔT**. This value is calculated as the subtraction of the mean age of the latter node (fig. 4, green dot) from the former's mean node age (fig. 4, D0, orange dot). The instant rates of evolution were retrieved from the output files of Phylobayes, these rates are computed by the software as described before (Kishino, et al. 2001; Lepage, et al. 2007) and are expressed as amino acid changes per site per unit of time. The rate at node D0 was termed $\mathbf{v_{max}}$ and a baseline rate of evolution during the Proterozoic was obtained as the average of all node rates in Group 4 D1 and D2 and denoted $\mathbf{v_{min}}$. All estimated divergence times for each node of each tree used in this analysis are provided in the supplementary data files.

Acknowledgements

This work was supported by an Imperial College London Junior Research Fellowship (T.C.), a Royal Society Dorothy Hodgkin Fellowship (P.S.-B.), the Biotechnology and Biological Sciences Research Council (BB/K002627/1 to A.W.R. and BB/L011206/1 to A.W.R.), and the Royal Society Wolfson Research Merit Award (A.W.R). The authors are immensely grateful to Prof. Euan Nisbet,

Prof. Donald E. Canfield, Prof. Minik Rosing, and Dr. Andrea Fantuzzi for valuable comments and feedback. Computing resources were provided by the HPC facility of Imperial College London.

References

Albalat R, Canestro C. 2016. Evolution by gene loss. Nature Rev Genet 17:379-391.

Battistuzzi FU, Hedges SB. 2009. A major clade of prokaryotes with ancient adaptations to life on land. Mol Biol Evol 26:335-343.

Beanland TJ. 1990. Evolutionary relationships between Q-Type photosynthetic reaction centers - Hypothesis-testing using parsimony. J Theor Biol 145:535-545.

Bekker A, Holland HD, Wang PL, Rumble D, 3rd, Stein HJ, Hannah JL, Coetzee LL, Beukes NJ. 2004. Dating the rise of atmospheric oxygen. Nature 427:117-120.

Blank CE, Sanchez-Baracaldo P. 2010. Timing of morphological and ecological innovations in the cyanobacteria - a key to understanding the rise in atmospheric oxygen. Geobiology 8:1-23.

Blankenship RE. 1992. Origin and early evolution of photosynthesis. Photosynth Res 33:91-111.

Bosak T, Liang B, Sim MS, Petroff AP. 2009. Morphological record of oxygenic photosynthesis in conical stromatolites. Proc Natl Acad Sci U S A 106:10939-10943.

Boucher Y, Douady CJ, Papke RT, Walsh DA, Boudreau ME, Nesbo CL, Case RJ, Doolittle WF. 2003. Lateral gene transfer and the origins of prokaryotic groups. Annu Rev Genet 37:283-328.

Brinkert K, De Causmaecker S, Krieger-Liszkay A, Fantuzzi A, Rutherford AW. 2016. Bicarbonate-induced redox tuning in Photosystem II for regulation and protection. Proc Natl Acad Sci U S A 113:12144-12149.

Brucker RM, Bordenstein SR. 2012. Speciation by symbiosis. Trends Ecol Evol 27:443-451.

Bryant D, Liu Z, LI T, Zhao F, Klatt CG, Ward D, Frigaard NU, Overmann J. 2012. Comparative and functional genomics of anoxygenic green bacteria from the taxa Chlorobi, Chloroflexi, and Acidobacteria. In: Burnap RL, Vermaas W, editors. Functional Genomics and Evolution of Photosynthetic Systems. Dordrecht Springer. p. 47-102.

Bukh J, Pietschmann T, Lohmann V, Krieger N, Faulk K, Engle RE, Govindarajan S, Shapiro M, Claire MS, Bartenschlager R. 2002. Mutations that permit efficient replication of hepatitis C virus RNA in Huh-7 cells prevent productive replication in chimpanzees. Proc Natl Acad Sci U S A 99:14416-14421.

Butterfield NJ. 2000. Bangiomorpha pubescens n. gen., n. sp.: implications for the evolution of sex, multicellularity, and the Mesoproterozoic/Neoproterozoic radiation of eukaryotes. Paleobiology 26:386-404.

Butterfield NJ. 2015. Proterozoic photosynthesis - a critical review. Palaeontology 58:953-972.

Canestro C, Albalat R, Hjelmqvist L, Godoy L, Jornvall H, Gonzalez-Duarte R. 2002. Ascidian and amphioxus adh genes correlate functional and molecular features of the ADH family expansion during vertebrate evolution. J Mol Evol 54:81-89.

Cardona T. 2015. A fresh look at the evolution and diversification of photochemical reaction centers. Photosynth Res 126:111-134.

Cardona T. 2016. Reconstructing the origin of oxygenic photosynthesis: Do assembly and photoactivation recapitulate evolution? Front Plant Sci 7:257.

Cardona T, Murray JW, Rutherford AW. 2015. Origin and evolution of water oxidation before the last common ancestor of the cyanobacteria. Mol Biol Evol 32:1310-1328.

Cardona T, Sedoud A, Cox N, Rutherford AW. 2012. Charge separation in Photosystem II: A comparative and evolutionary overview. Biochim Biophys Acta 1817:26-43.

Carrat F, Flahault A. 2007. Influenza vaccine: The challenge of antigenic drift. Vaccine 25:6852-6862.

Ciccarelli FD, Doerks T, von Mering C, Creevey CJ, Snel B, Bork P. 2006. Toward automatic reconstruction of a highly resolved tree of life. Science 311:1283-1287.

Clarke JT, Warnock RCM, Donoghue PCJ. 2011. Establishing a time-scale for plant evolution. New Phytol 192:266-301.

Cockell CS. 2000. Ultraviolet radiation and the photobiology of earth's early oceans. Orig Life Evol Biosph 30:467-499.
Cogdell RJ, Howard TD, Bittl R, Schlodder E, Geisenheimer I, Lubitz W. 2000. How carotenoids protect bacterial photosynthesis. Philos Trans R Soc Lond B Biol Sci 355:1345-1349.
Cornejo-Castillo FM, Cabello AM, Salazar G, Sanchez-Baracaldo P, Lima-Mendez G, Hingamp P, Alberti A, Sunagawa S, Bork P, de Vargas C, et al. 2016. Cyanobacterial symbionts diverged in the late Cretaceous towards lineage-specific nitrogen fixation factories in single-celled phytoplankton. Nat Commun 7:11071.
Crawford TS, Hanning KR, Chua JP, Eaton-Rye JJ, Summerfield TC. 2016. Comparison of D1 - and D1-containing PS II reaction centre complexes under different environmental conditions in Synechocystis sp. PCC 6803. Plant Cell Environ 39:1715-1726.
Czaja AD, Johnson CM, Beard BL, Roden EE, Li WQ, Moorbath S. 2013. Biological Fe oxidation controlled deposition of banded iron formation in the ca. 3770 Ma Isua Supracrustal Belt (West Greenland). Earth Planet Sci Lett 363:192-203.
D'Souza G, Waschina S, Pande S, Bohl K, Kaleta C, Kost C. 2014. Less is more: Selective advantages can explain the prevalent loss of biosynthetic genes in bacteria. Evolution 68:2559-2570.
David LA, Alm EJ. 2011. Rapid evolutionary innovation during an Archaean genetic expansion. Nature 469:93-96.
De Las Rivas J, Balsera M, Barber J. 2004. Evolution of oxygenic photosynthesis: genome-wide analysis of the OEC extrinsic proteins. Trends Plant Sci 9:18-25.
Debus RJ. 2001. Amino acid residues that modulate the properties of tyrosine Y-Z and the manganese cluster in the water oxidizing complex of photosystem II. Biochim Biophys Acta 1503:164-186.
Deisenhofer J, Michel H. 1989. Nobel lecture. The photosynthetic reaction centre from the purple bacterium Rhodopseudomonas viridis. EMBO J 8:2149-2170.
Delwiche CF, Palmer JD. 1996. Rampant horizontal transfer and duplication of rubisco genes in eubacteria and plastids. Mol Biol Evol 13:873-882.
Di Rienzi SC, Sharon I, Wrighton KC, Koren O, Hug LA, Thomas BC, Goodrich JK, Bell JT, Spector TD, Banfield JF, et al. 2013. The human gut and groundwater harbor non-photosynthetic bacteria belonging to a new candidate phylum sibling to Cyanobacteria. Elife 2:e01102.
Dobakova M, Tichy M, Komenda J. 2007. Role of the PsbI protein in photosystem II assembly and repair in the cyanobacterium Synechocystis sp PCC 6803. Plant Physiol 145:1681-1691.
Dutton PL, Leight JS, Seibert M. 1972. Primary processes in photosynthesis: in situ ESR studies on the light induced oxidized and triplet state of reaction center bacteriochlorophyll. Biochem Biophys Res Commun 46:406-413.
Falcon LI, Magallon S, Castillo A. 2010. Dating the cyanobacterial ancestor of the chloroplast. ISME J 4:777-783.
Feng DF, Cho G, Doolittle RF. 1997. Determining divergence times with a protein clock: update and reevaluation. Proc Natl Acad Sci U S A 94:13028-13033.
Ferreira KN, Iverson TM, Maghlaoui K, Barber J, Iwata S. 2004. Architecture of the photosynthetic oxygen-evolving center. Science 303:1831-1838.
Fischer WW, Hemp J, Johnson JE. 2016. Evolution of oxygenic photosynthesis. Annu Rev Earth Planet Sci 44:647-683.
Franzen LG, Hansson O, Andreasson LE. 1985. The roles of the extrinsic subunits in Photosystem II as revealed by Electron Paramagnetic Resonance. Biochim Biophys Acta 808:171-179.
Frei R, Crowe SA, Bau M, Polat A, Fowle DA, Døssing LN. 2016. Oxidative elemental cycling under the low O_2 Eoarchean atmosphere. Sci Rep 6:21058.
Georgelis N, Braun EL, Hannah LC. 2008. Duplications and functional divergence of ADP-glucose pyrophosphorylase genes in plants. BMC Evol Biol 8.
Golubic S, Lee SJ. 1999. Early cyanobacterial fossil record: preservation, palaeoenvironments and identification. Ur J Phycol 34:339-348.
Golubic S, Sergeev VN, Knoll AH. 1995. Mesoproterozoic Archaeoellipsoides: Akinetes of heterocystous cyanobacteria. Lethaia 28:285-298.
Grassineau NV, Abell PI, Appel PWU, Lowry D, Nisbet EG. 2006. Early life signatures in sulfur and carbon isotopes from Isua, Barberton, Wabigoon (Steep Rock), and Belingwe Greenstone Belts (3.8 to 2.7 Ga). Geol Soc Am Mem 198:33-52.

Guindon S, Dufayard JF, Lefort V, Anisimova M, Hordijk W, Gascuel O. 2010. New algorithms and methods to estimate maximum-likelihood phylogenies: assessing the performance of PhyML 3.0. Syst Biol 59:307-321.
Harel A, Karkar S, Cheng S, Falkowski PG, Bhattacharya D. 2015. Deciphering primordial cyanobacterial genome functions from protein network analysis. Curr Biol 25:628-634.
Ho MY, Shen G, Canniffe DP, Zhao C, Bryant DA. 2016. Light-dependent chlorophyll *f* synthase is a highly divergent paralog of PsbA of photosystem II. Science 353.
Ho SYW, Duchene S. 2014. Molecular-clock methods for estimating evolutionary rates and timescales. Mol Ecol 23:5947-5965.
Honda D, Yokota A, Sugiyama J. 1999. Detection of seven major evolutionary lineages in cyanobacteria based on the 16S rRNA gene sequence analysis with new sequences of five marine Synechococcus strains. J Mol Evol 48:723-739.
Huang Y, Zeng Y, Lu H, Feng H, Zeng Y, Koblizek M. 2016. Novel *acsF* gene primers revealed a diverse phototrophic bacterial population, including Gemmatimonadetes, in Lake Taihu (China). Appl Environ Microbiol 82:5587-5594.
Igarashi N, Harada J, Nagashima S, Matsuura K, Shimada K, Nagashima KV. 2001. Horizontal transfer of the photosynthesis gene cluster and operon rearrangement in purple bacteria. J Mol Evol 52:333-341.
Jia YT, Dewey G, Shindyalov IN, Bourne PE. 2004. A new scoring function and associated statistical significance for structure alignment by CE. J Comp Biol 11:787-799.
Jun SR, Sims GE, Wu GHA, Kim SH. 2010. Whole-proteome phylogeny of prokaryotes by feature frequency profiles: An alignment-free method with optimal feature resolution. Proc Natl Acad Sci U S A 107:133-138.
Kagan RM, McFadden HJ, McFadden PN, OConnor C, Clarke S. 1997. Molecular phylogenetics of a protein repair methyltransferase. Comp Biochem Physiol B Biochem Mol Biol 117:379-385.
Kay EH, Hoekstra HE. 2008. Rodents. Curr Biol 18:R406-R410.
Khadka B, Adeolu M, Blankenship RE, Gupta RS. 2017. Novel insights into the origin and diversification of photosynthesis based on analyses of conserved indels in the core reaction center proteins. Photosynth Res 131:159-171.
Kim H, Li H, Maresca JA, Bryant DA, Savikhin S. 2007. Triplet exciton formation as a novel photoprotection mechanism in chlorosomes of *Chlorobium tepidum*. Biophys J 93:192-201.
Kishino H, Thorne JL, Bruno WJ. 2001. Performance of a divergence time estimation method under a probabilistic model of rate evolution. Mol Biol Evol 18:352-361.
Klatt CG, Wood JM, Rusch DB, Bateson MM, Hamamura N, Heidelberg JF, Grossman AR, Bhaya D, Cohan FM, Kuhl M, et al. 2011. Community ecology of hot spring cyanobacterial mats: predominant populations and their functional potential. ISME J 5:1262-1278.
Knoll AH. 2015. Paleobiological perspectives on early microbial evolution. Cold Spring Harb Perspect Biol 7:a018093.
Knoll AH, Worndle S, Kah LC. 2013. Covariance of microfossil assemblages and microbialite textures across an upper mesoproterozoic carbonate platform. Palaios 28:453-470.
Komenda J, Sobotka R, Nixon PJ. 2012. Assembling and maintaining the Photosystem II complex in chloroplasts and cyanobacteria. Curr Opin Plant Biol 15:245-251.
Komenda J, Tichy M, Prasil O, Knoppova J, Kuvikova S, de Vries R, Nixon PJ. 2007. The exposed N-terminal tail of the D1 subunit is required for rapid D1 degradation during photosystem II repair in *Synechocystis* sp PCC 6803. Plant Cell 19:2839-2854.
Koskiniemi S, Sun S, Berg OG, Andersson DI. 2012. Selection-driven gene loss in bacteria. PLoS Genet 8:e1002787.
Koyama K, Suzuki H, Noguchi T, Akimoto S, Tsuchiya T, Mimuro M. 2008. Oxygen evolution in the thylakoid-lacking cyanobacterium *Gloeobacter violaceus* PCC 7421. Biochim Biophys Acta 1777:369-378.
Krieger-Liszkay A, Fufezan C, Trebst A. 2008. Singlet oxygen production in photosystem II and related protection mechanism. Photosynth Res 98:551-564.
Krynicka V, Shao S, Nixon PJ, Komenda J. 2015. Accessibility controls selective degradation of photosystem II subunits by FtsH protease. Nat Plants 1:15168.

Ku C, Nelson-Sathi S, Roettger M, Sousa FL, Lockhart PJ, Bryant D, Hazkani-Covo E, McInerney JO, Landan G, Martin WF. 2015. Endosymbiotic origin and differential loss of eukaryotic genes. Nature 524:427-432.

Lancaster CRD, Michel H. 1997. The coupling of light-induced electron transfer and proton uptake as derived from crystal structures of reaction centres from *Rhodopseudomonas viridis* modified at the binding site of the secondary quinone, Q_B. Structure 5:1339-1359.

Lartillot N, Lepage T, Blanquart S. 2009. PhyloBayes 3: a Bayesian software package for phylogenetic reconstruction and molecular dating. Bioinformatics 25:2286-2288.

Lartillot N, Philippe H. 2004. A Bayesian mixture model for across-site heterogeneities in the amino-acid replacement process. Mol Biol Evol 21:1095-1109.

Lepage T, Bryant D, Philippe H, Lartillot N. 2007. A general comparison of relaxed molecular clock models. Mol Biol Evol 24:2669-2680.

Lewis CA, Crayle J, Zhou ST, Swanstrom R, Wolfenden R. 2016. Cytosine deamination and the precipitous decline of spontaneous mutation during Earth's history. Proc Natl Acad Sci U S A 113:8194-8199.

Linke K, Ho FM. 2013. Water in Photosystem II: Structural, functional and mechanistic considerations. Biochim Biophys Acta 1837:14-32.

Lyons TW, Reinhard CT, Planavsky NJ. 2014. The rise of oxygen in Earth's early ocean and atmosphere. Nature 506:307-315.

Magnuson A, Cardona T. 2016. Thylakoid membrane function in heterocysts. Biochim Biophys Acta 1857:309-319.

Marin J, Battistuzzi FU, Brown AC, Hedges SB. 2017. The timetree of prokaryotes: New insights into their evolution and speciation. Mol Biol Evol 34:437-446.

Matsunami M, Yoshioka T, Minoura T, Okano Y, Muto Y. 2011. Evolutionary features and intracellular behavior of the PRTB protein. Biochem Genet 49:458-473.

Melo TB, Frigaard NU, Matsuura K, Naqvi KR. 2000. Electronic energy transfer involving carotenoid pigments in chlorosomes of two green bacteria: *Chlorobium tepidum* and *Chloroflexus aurantiacus*. Spectrochim Acta Mol Biomol Spectrosc 56:2001-2010.

Michel H, Deisenhofer J. 1988. Relevance of the photosynthetic reaction center from purple bacteria to the structure of Photosystem II. Biochemistry 27:1-7.

Moore RB, Obornik M, Janouskovec J, Chrudimsky T, Vancova M, Green DH, Wright SW, Davies NW, Bolch CJ, Heimann K, et al. 2008. A photosynthetic alveolate closely related to apicomplexan parasites. Nature 451:959-963.

Mulkidjanian AY, Koonin EV, Makarova KS, Mekhedov SL, Sorokin A, Wolf YI, Dufresne A, Partensky F, Burd H, Kaznadzey D, et al. 2006. The cyanobacterial genome core and the origin of photosynthesis. Proc Natl Acad Sci U S A 103:13126-13131.

Murray JW. 2012. Sequence variation at the oxygen-evolving centre of photosystem II: a new class of 'rogue' cyanobacterial D1 proteins. Photosynth Res 110:177-184.

Nakamura Y, Kaneko T, Sato S, Mimuro M, Miyashita H, Tsuchiya T, Sasamoto S, Watanabe A, Kawashima K, Kishida Y, et al. 2003. Complete genome structure of *Gloeobacter violaceus* PCC 7421, a cyanobacterium that lacks thylakoids. DNA Research 10:137-145.

Nakayama T, Kamikawa R, Tanifuji G, Kashiyama Y, Ohkouchi N, Archibald JM, Inagaki Y. 2014. Complete genome of a nonphotosynthetic cyanobacterium in a diatom reveals recent adaptations to an intracellular lifestyle. Proc Natl Acad Sci U S A 111:11407-11412.

Nickelsen J, Rengstl B. 2013. Photosystem II Assembly: From Cyanobacteria to Plants. Annu Rev Plant Biol 64:609-635.

Nisbet EG, Fowler CFR. 2014. The early history of life. In: M. KD, Schlesinger WH, editors. Treatise on Geochemistry. Amsterdam: Elsevier Science. p. 1-42.

Nitschke W, Rutherford AW. 1991. Photosynthetic reaction centers - Variations on a common structural theme. Trends Biochem Sci 16:241-245.

Niwa S, Yu LJ, Takeda K, Hirano Y, Kawakami T, Wang-Otomo ZY, Miki K. 2014. Structure of the LH1-RC complex from *Thermochromatium tepidum* at 3.0 A. Nature 508:228-232.

Nixon PJ, Diner BA. 1994. Analysis of water-oxidation mutants constructed in the cyanobacterium *Synechocystis* sp. PCC 6803. Biochem Soc Trans 22:338-343.

Nixon PJ, Michoux F, Yu JF, Boehm M, Komenda J. 2010. Recent advances in understanding the assembly and repair of photosystem II. Ann Bot 106:1-16.
Nutman AP, Bennett VC, Friend CRL, Van Kranendonk MJ, Chivas AR. 2016. Rapid emergence of life shown by discovery of 3,700-million-year-old microbial structures. Nature 537:535:538.
Planavsky NJ, Asael D, Hofmann A, Reinhard CT, Lalonde SV, Knudsen A, Wang X, Ossa Ossa F, Pecoits E, Smith AJB, et al. 2014. Evidence for oxygenic photosynthesis half a billion years before the Great Oxidation Event. Nature Geosci 7:283-286.
Ravin NV, Gruzdev EV, Beletsky AV, Mazur AM, Prokhortchouk EB, Filyushin MA, Kochieva EZ, Kadnikov VV, Mardanov AV, Skryabin KG. 2016. The loss of photosynthetic pathways in the plastid and nuclear genomes of the non-photosynthetic mycoheterotrophic eudicot *Monotropa hypopitys*. BMC Plant Biol 16:238.
Raymond J. 2009. The role of horizontal gene transfer in photosynthesis, oxygen production, and oxygen tolerance. Methods Mol Biol 532:323-338.
Riding R, Fralick P, Liang LY. 2014. Identification of an Archean marine oxygen oasis. Precambrian Research 251:232-237.
Rinke C, Schwientek P, Sczyrba A, Ivanova NN, Anderson IJ, Cheng JF, Darling A, Malfatti S, Swan BK, Gies EA, et al. 2013. Insights into the phylogeny and coding potential of microbial dark matter. Nature 499:431-437.
Roose JL, Frankel LK, Mummadisetti MP, Bricker TM. 2016. The extrinsic proteins of photosystem II: update. Planta 243:889-908.
Rosing MT. 1999. C-13-depleted carbon microparticles in > 3700-Ma sea-floor sedimentary rocks from west Greenland. Science 283:674-676.
Rosing MT, Frei R. 2004. U-rich Archaean sea-floor sediments from Greenland - indications of > 3700 Ma oxygenic photosynthesis. Earth Planet Sci Lett 217:237-244.
Rutherford AW. 1989. Photosystem II, the water-splitting enzyme. Trends in Biochemical Sciences 14:227-232.
Rutherford AW, Faller P. 2003. Photosystem II: evolutionary perspectives. Philos Trans R Soc Lond B Biol Sci 358:245-253.
Rutherford AW, Nitschke W. 1996. Photosystem II and the quinone–iron-containing reaction centers. In: Baltscheffsky H, editor. Origin and evolution of biological energy conversion. New York, N. Y.: VCH. p. 143–175.
Rutherford AW, Osyczka A, Rappaport F. 2012. Back-reactions, short-circuits, leaks and other energy wasteful reactions in biological electron transfer: redox tuning to survive life in O_2. FEBS Lett 586:603-616.
Rutherford AW, Paterson DR, Mullet JE. 1981. A light-induced spin-polarized triplet detected by EPR in photosystem II reaction centers. Biochim Biophys Acta 635:205-214.
Sadekar S, Raymond J, Blankenship RE. 2006. Conservation of distantly related membrane proteins: Photosynthetic reaction centers share a common structural core. Mol Biol Evol 23:2001-2007.
Sanchez-Baracaldo P. 2015. Origin of marine planktonic cyanobacteria. Sci Rep 5:17418.
Sanchez-Baracaldo P, Hayes PK, Blank CE. 2005. Morphological and habitat evolution in the Cyanobacteria using a compartmentalization approach. Geobiology 3:145-165.
Satkoski AM, Beukes NJ, Li W, Beard BL, Johnson CM. 2015. A redox-stratified ocean 3.2 billion years ago. Earth Planet Sci Lett 430:43-53.
Saw JHW, Schatz M, Brown MV, Kunkel DD, Foster JS, Shick H, Christensen S, Hou SB, Wan XH, Donachie SP. 2013. Cultivation and complete genome sequencing of *Gloeobacter kilaueensis* sp nov., from a lava cave in Kilauea Caldera, Hawai'i. PLoS One 8:e76376.
Schidlowski M. 1988. A 3,800-Million-Year Isotopic Record of Life from Carbon in Sedimentary-Rocks. Nature 333:313-318.
Schirrmeister BE, de Vos JM, Antonelli A, Bagheri HC. 2013. Evolution of multicellularity coincided with increased diversification of cyanobacteria and the Great Oxidation Event. Proc Natl Acad Sci U S A 110:1791-1796.
Schirrmeister BE, Gugger M, Donoghue PCJ. 2015. Cyanobacteria and the Great Oxidation Event: evidence from genes and fossils. Palaeontology 58:769-785.
Schirrmeister BE, Sanchez-Baracaldo P, Wacey D. 2016. Cyanobacterial evolution during the Precambrian. Int J Astrobiol 15:187-204.

Segata N, Bornigen D, Morgan XC, Huttenhower C. 2013. PhyloPhlAn is a new method for improved phylogenetic and taxonomic placement of microbes. Nat Commun 4:2304.
Sergeev VN, Gerasimenko LM, Zavarzin GA. 2002. Proterozoic history and present state of cyanobacteria. Mikrobiologiia 71:725-740.
Shih PM, Hemp J, Ward LM, Matzke NJ, Fischer WW. 2017. Crown group Oxyphotobacteria postdate the rise of oxygen. Geobiology 15:19-29.
Shih PM, Wu D, Latifi A, Axen SD, Fewer DP, Talla E, Calteau A, Cai F, Tandeau de Marsac N, Rippka R, et al. 2013. Improving the coverage of the cyanobacterial phylum using diversity-driven genome sequencing. Proc Natl Acad Sci U S A 110:1053-1058.
Sicora CI, Ho FM, Salminen T, Styring S, Aro EM. 2009. Transcription of a "silent" cyanobacterial *psbA* gene is induced by microaerobic conditions. Biochim Biophys Acta 1787:105-112.
Sievers F, Wilm A, Dineen D, Gibson TJ, Karplus K, Li WZ, Lopez R, McWilliam H, Remmert M, Soding J, et al. 2011. Fast, scalable generation of high-quality protein multiple sequence alignments using Clustal Omega. Mol Syst Biol 7:539.
Sims PA, Mann DG, Medlin LK. 2006. Evolution of the diatoms: insights from fossil, biological and molecular data. Phycologia 45:361-402.
Soo RM, Skennerton CT, Sekiguchi Y, Imelfort M, Paech SJ, Dennis PG, Steen JA, Parks DH, Tyson GW, Hugenholtz P. 2014. An expanded genomic representation of the phylum Cyanobacteria. Genome Biol Evol 6:1031-1045.
Soo RM, Woodcroft BJ, Parks DH, Tyson GW, Hugenholtz P. 2015. Back from the dead; the curious tale of the predatory cyanobacterium *Vampirovibrio chlorellavorus*. PeerJ 3:e968.
Sousa FL, Shavit-Grievink L, Allen JF, Martin WF. 2013. Chlorophyll biosynthesis gene evolution indicates photosystem gene duplication, not photosystem merger, at the origin of oxygenic photosynthesis. Genome Biol Evol 5:200-216.
Suga M, Akita F, Hirata K, Ueno G, Murakami H, Nakajima Y, Shimizu T, Yamashita K, Yamamoto M, Ago H, et al. 2015. Native structure of photosystem II at 1.95 angstrom resolution viewed by femtosecond X-ray pulses. Nature 517:99-U265.
Sugiura M, Nakamura M, Koyama K, Boussac A. 2015. Assembly of oxygen-evolving Photosystem II efficiently occurs with the apo-Cytb(559) but the holo-Cytb(559) accelerates the recovery of a functional enzyme upon photoinhibition. Biochim Biophys Acta 1847:276-285.
Sullivan MB, Lindell D, Lee JA, Thompson LR, Bielawski JP, Chisholm SW. 2006. Prevalence and evolution of core photosystem II genes in marine cyanobacterial viruses and their hosts. Plos Biology 4:1344-1357.
Swingley WD, Blankenship RE, Raymond J. 2009. Evolutionary relationships among purple photosynthetic bacteria and the origin of proteobacterial photosynthetic systems. In: Hunter CN, Daldal F, Thurnauer MC, T. BJ, editors. The Purple Phototrophic Bacteria. Netherlands: Springer. p. 17-29.
Tank M, Thiel V, Imhoff JF. 2009. Phylogenetic relationship of phototrophic purple sulfur bacteria according to *pufL* and *pufM* genes. Int Microbiol 12:175-185.
Thompson AW, Foster RA, Krupke A, Carter BJ, Musat N, Vaulot D, Kuypers MMM, Zehr JP. 2012. Unicellular cyanobacterium symbiotic with a single-celled eukaryotic alga. Science 337:1546-1550.
Tice MM, Lowe DR. 2004. Photosynthetic microbial mats in the 3,416-Myr-old ocean. Nature 431:549-552.
Tsukatani Y, Romberger SP, Golbeck JH, Bryant DA. 2012. Isolation and characterization of homodimeric Type-I reaction center complex from *Candidatus* Chloracidobacterium thermophilum, an aerobic chlorophototroph. J Biol Chem 287:5720-5732.
Umena Y, Kawakami K, Shen JR, Kamiya N. 2011. Crystal structure of oxygen-evolving photosystem II at a resolution of 1.9 A. Nature 473:55-60.
Vass I, Cser K. 2009. Janus-faced charge recombinations in photosystem II photoinhibition. Trends Plant Sci 14:200-205.
Ward LM, Kirschvink JL, Fischer WW. 2016. Timescales of oxygenation following the evolution of oxygenic photosynthesis. Orig Life Evol Biosph 46:51-65.

Wegener KM, Nagarajan A, Pakrasi HB. 2015. An atypical psbA gene encodes a sentinel D1 protein to form a physiologically relevant inactive photosystem II complex in cyanobacteria. J Biol Chem 290:3764-3774.

Weiss MC, Sousa FL, Mrnjavac N, Neukirchen S, Roettger M, Nelson-Sathi S, Martin WF. 2016. The physiology and habitat of the last universal common ancestor. Nat Microbiol 1:16116.

Wu D, Hugenholtz P, Mavromatis K, Pukall R, Dalin E, Ivanova NN, Kunin V, Goodwin L, Wu M, Tindall BJ, et al. 2009. A phylogeny-driven genomic encyclopaedia of Bacteria and Archaea. Nature 462:1056-1060.

Xiao S, Knoll AH, Yuan X, Pueschel CM. 2004. Phosphatized multicellular algae in the Neoproterozoic Doushantuo Formation, China, and the early evolution of florideophyte red algae. Am J Bot 91:214-227.

Xiong J, Inoue K, Bauer CE. 1998. Tracking molecular evolution of photosynthesis by characterization of a major photosynthesis gene cluster from Heliobacillus mobilis. Proc Natl Acad Sci U S A 95:14851-14856.

Yang Z, Rannala B. 2006. Bayesian estimation of species divergence times under a molecular clock using multiple fossil calibrations with soft bounds. Mol Biol Evol 23:212-226.

Zeng YH, Feng FY, Medova H, Dean J, Koblizek M. 2014. Functional Type 2 photosynthetic reaction centers found in the rare bacterial phylum Gemmatimonadetes. Proc Natl Acad Sci U S A 111:7795-7800.

Figure legends

Fig. 1. Schematic representation of the evolution of Type II reaction centers. (*a*) All reaction centers have common ancestry and descended from a homodimeric reaction center, marked **A**. From **A**, two new reaction centers emerged, one ancestral to all Type II reaction centers (**II**) and a second ancestral to all Type I reaction centers. This is the earliest diversification event of reaction center proteins that can be inferred from sequence and structural data and it is marked **1**. The ancestral Type II reaction center protein (**II**) gave rise to two new proteins, one ancestral to D1 and D2, named **D0** and a second ancestral to L and M named **K**. The ancestral L and M subunits further diversify into Chloroflexi-type and Proteobacteria-type L and M subunits (**5**). Step **6** indicates that Type I reaction center proteins also diversified in parallel to Type II reaction center proteins. (*b*) Evolution of cyanobacterial D1 and D2, modified from Cardona, et al. (2015). The conserved structural and functional traits between D1 and D2 indicate that the ancestral homodimeric photosystem was able to oxidize water, this is represented by a fuchsia spot in each D0 monomer. However, ancestral reconstructions of **D0** suggest that the primordial catalytic cluster was not identical to that of standard D1, but may have been slightly modified. The blue border around the fuchsia spot indicates that the ancestral standard D1 is the earliest point where the current configuration of the Mn_4CaO_5 cluster can be traced back from available sequence data. **ΔT** marks the span of time between D0 and the appearance of the ancestral standard form of D1

Fig. 2. Structural comparisons of Type II reaction center proteins. (*a*) Four conserved structural domains are shared by D1 and D2 not present in L and M: these are highlighted in orange and marked from 1 to 4 and their functions are described in the text. These four structural domains are required to support water oxidation, repair, assembly, and photoprotection. D1 and D2 are from the crystal structure of PSII from *Thermosynechococcus vulcanus*, PDB: 3WU2 (Umena, et al. 2011) and L and M from *Thermochromatium tepidum*, PDB: 3WMM (Niwa, et al. 2014). (*b*) Structure of the Mn_4CaO_5 cluster in D1 and the corresponding site in D2. The residues colored in grey are provided by D1 and D2 protein and those colored in orange by CP43 and CP47. Notice that while a redox Y-H pair is conserved in D1 and D2, D2/CP47 evolved to stop the binding of metals by replacing ligands for phenylalanine residues creating a hydrophobic patch. Such a site is not found in any other Type II or Type I reaction center protein and it is unique to D2 (Cardona, et al. 2015). (*c*) Overlap of D1 and D2 highlighting some of the conserved traits as described in the text

Fig. 3. Decrease of sequence identity of D1 and D2 proteins as a function of divergence time. D1 subunits are shown in grey and D2 in orange. The divergence time between pairs of species is plotted against the level of sequence identity as tabulated in supplementary table S1. The red circle, placed at 79.2% corresponds to the average of sequence identity of the three distinct Group 4 D1 sequences of *Gloeobacter violaceous* in comparison with that of *Cyanidioschyzon merolae*. The light orange bar

marks the GOE. The dashed line is fitted from a linear function and shows that over a period of about 2.0 Ga no dramatic changes in the rates of evolution of D1 and D2 are observed. It also shows that a constant rate of evolution (strict clock) is unlikely across all times. Fit parameters are shown in supplementary table S2. The pink box around 3.5-3.8 Ga marks the likeliest location for the earliest events in the history of photosynthesis, that is the divergence of D1 and D2 (~27% sequence identity), the divergence of anoxygenic (L/M) and oxygenic (D1/D2) reaction center proteins (~17%), and the divergence of Type I and Type II reaction center proteins (≤5%)

Fig. 4. Molecular clock analysis of Type II reaction center proteins. A log-normal autocorrelated relaxed clock is shown implementing a CAT + GTR + Γ non-parametric model with flexible boundaries on the calibration points. Red dots are calibration points as described in Materials and Methods. The grey dot denoted II, represents the ancestral Type II reaction center protein, as schematized in fig. 1A. The orange dot (D0) marks the initial divergence of D1 and D2. The violet dot marks the divergence point between G2 atypical D1 sequences and standard D1. The green dot marks the divergence point between the microaerobic D1 forms (G3) and the dominant form of D1 (G4). This point represents the last common ancestral protein to all standard D1 forms known to have a complete ligand sphere to the Mn_4CaO_5 cluster. The blue dot represents the origin of the dominant form of D1 inherited by all extant Cyanobacteria and photosynthetic eukaryotes. The grey bars represent the standard error of the estimated divergence times at the nodes. The orange bar shows the GOE

Fig. 5. Rates of evolution as a function of time. (*a*) Change in the rate of evolution of oxygenic (grey) and anoxygenic (orange) Type II reaction center proteins. The rates were obtained from the tree in fig. 4, which was calculated using a root prior of 3.5 ± 0.05 Ga. The dashed lines represent a fit of a single-component exponential decay and the rates are given as amino acid substitutions per site per million years. The fit components are shown in supplementary table S4. (*b*) Rate of evolution of D1 and D2 nodes with changed root priors, the red curve farthest to the right was calculated using a root prior of 4.2 ± 0.05 Ga, while the green curve farthest to the left was calculated using a root prior of 0.8 ± 0.05 Ga. (*c*) Change in the rate of evolution as a function of **ΔT**, the dashed lines represents a fit to a power-law function. The fit components are shown in supplementary table S5

Fig. 6. Effect of evolutionary models on estimated divergence times. (*a*) Effect of equilibrium frequencies: the *y* axis represent estimated divergence times calculated with a CAT + GTR model while those in the *x* axis with a CAT model with uniform equilibrium frequencies (Poisson), see also supplementary fig. S1 for additional model comparisons. (*b*) Effect of Calibration on the estimated divergence time: the estimated divergence times in the *y* axis were calculated using a calibration point 11 with a minimum age of 2.45 Ga, while those in the *x* axis using a minimum age of 2.70 Ga (see

Materials and Methods), both trees were ran under a CAT model with uniform equilibrium frequencies. See also supplementary fig. S2 for additional model comparisons. (*c*) Effect of the model of evolutionary rate variation: the estimated divergence times in the *y* axis were calculated using an uncorrelated gamma model, while those in the *x* axis using an autocorrelated log normal model, both trees were ran under a CAT model with uniform equilibrium frequencies. See also supplementary fig. S3 for additional model comparisons. In each case the root prior was 3.5 ± 0.05 Ga

Tables

Table 1. Effect on **ΔT** assuming different ages for the most ancestral Type II reaction center protein

Root prior	II	D0	Ancestral standard D1	ΔT
		CAT + GTR + Γ		
3.2	3.25 ± 0.05	2.80 ± 0.16	1.99 ± 0.19	0.80
3.5	3.54 ± 0.05	3.22 ± 0.19	2.19 ± 0.24	1.02
3.8	3.83 ± 0.05	3.44 ± 0.21	2.27 ± 0.24	1.17
4.1	4.12 ± 0.05	3.71 ± 0.23	2.38 ± 0.25	1.32
		LG + Γ		
3.2	3.27 ± 0.05	3.19 ± 0.08	2.51 ± 0.13	0.68
3.5	3.53 ± 0.05	3.40 ± 0.09	2.64 ± 0.15	0.77
3.8	3.81 ± 0.05	3.64 ± 0.12	2.77 ± 0.17	0.88
4.1	4.10 ± 0.05	3.91 ± 0.14	2.90 ± 0.19	1.01

Table 2. Comparison of rates of protein evolution

	Rate Amino acid substitutions per site per Ga	Citations
D0 (ν_{max})	5.03	This work[a]
Group 4 D1 and D2 (ν_{min})	0.12	This work[a]
K	6.11	This work[a]
L and M	0.40	This work[a]
ADP-glucose pyrophosphorylase large subunit (plants)	1.2	(Georgelis, et al. 2008)
PRTB Protein[b] (humans)	0.13	(Matsunami, et al. 2011)
Alcohol dehydrogenase (ascidians)	0.27	(Canestro, et al. 2002)
Protein-L-isoaspartyl (D-aspartyl) *O*-methyltransferase (bacteria to humans[c])	0.39	(Kagan, et al. 1997)
Hepatitis C Virus	3700	(Bukh, et al. 2002)
Influenza virus type A (H1)	5800	(Carrat and Flahault 2007)

[a]Estimated using a root prior of 3.5 Ga under a autocorrelated log-normal molecular clock as described in the text and Material and Methods.

[b]Proline-rich transcript overexpressed in the brain (PRTB). The human protein shares 99% sequence identity compared to that in mice. Rodents are estimated to have diverged by 74 Ma (Kay and Hoekstra 2008).
[c]The authors pointed out that the rate of evolution of this methyltransferase has remain unchanged from bacteria to humans.

Table 3. Change in **ΔT** under different evolutionary models

Model	Root prior (Ga)	Calibration (Ga)	ΔT (Ga)
CAT + GTR (autoc.[a])	3.5	2.45	1.02
CAT + GTR (autoc.)	3.5	2.70	0.97
CAT + GTR (autoc.)	3.8	2.45	1.19
CAT + GTR (autoc.)	3.8	2.70	1.13
CAT + Pois. (autoc.)	3.5	2.45	1.02
CAT + Pois. (autoc.)	3.5	2.70	1.00
CAT + Pois. (autoc.)	3.8	2.45	1.17
CAT + Pois. (autoc.)	3.8	2.70	1.12
CAT + Pois. (uncor.[b])	3.5	2.45	1.94
CAT + Pois. (uncor.)	3.5	2.70	1.84
CAT + Pois. (uncor.)	3.8	2.45	1.67
CAT + Pois. (uncor.)	3.8	2.70	2.03

[a]Log normal autocorrelated clock model.
[b]Uncorrelated gamma model

Table 4. Calibration points

Node	Event	Maximum age (Ma)	Minimum age (Ma)
1	*Arabidopsis-Populus* divergence	127	82
2	Angiosperms	248	124
3	Gymnosperms	366	306
4	Land plants	-	475
5	Diatoms-Coscinodiscophyceae	-	190
6	Floridiophyceae	-	600
7	Rhodophyta	-	1222
8	Nostocales	1900	1600
9	Pleurocapsales	-	1700
10	First occurrence of multicellularity	-	1900
11	*G. violaceous* divergence on D2 and on Group 4 D1	-	2450 (Cal. 1) 2700 (Cal. 2)

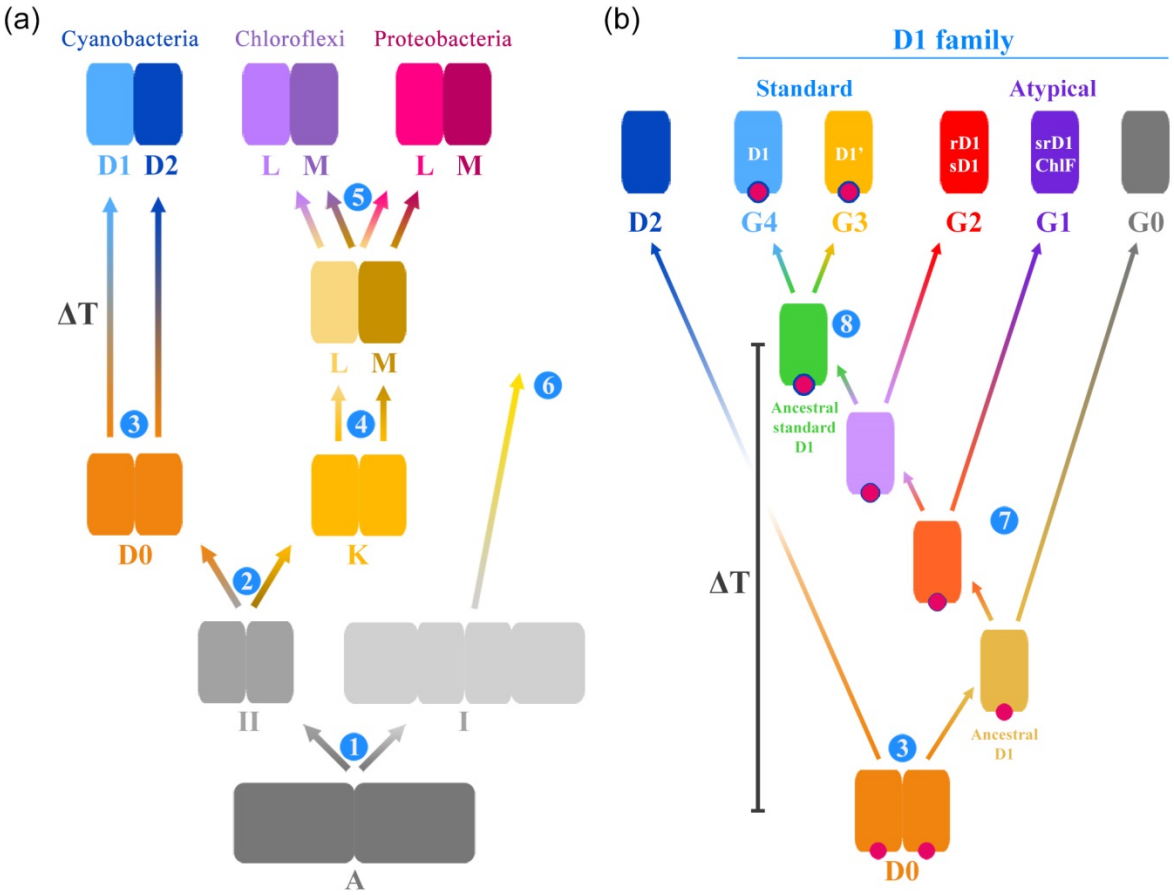
(a)
Cyanobacteria
Chloroflexi
Proteobacteria
D1 D2
L M
L M
ΔT
L M
D0
K
II
I
A
(b)
D1 family
Standard
Atypical
D1
D1'
rD1
sD1
srD1
ChlF
D2
G4
G3
G2
G1
G0
Ancestral
standard
D1
ΔT
Ancestral
D1
D0

Fig. 1

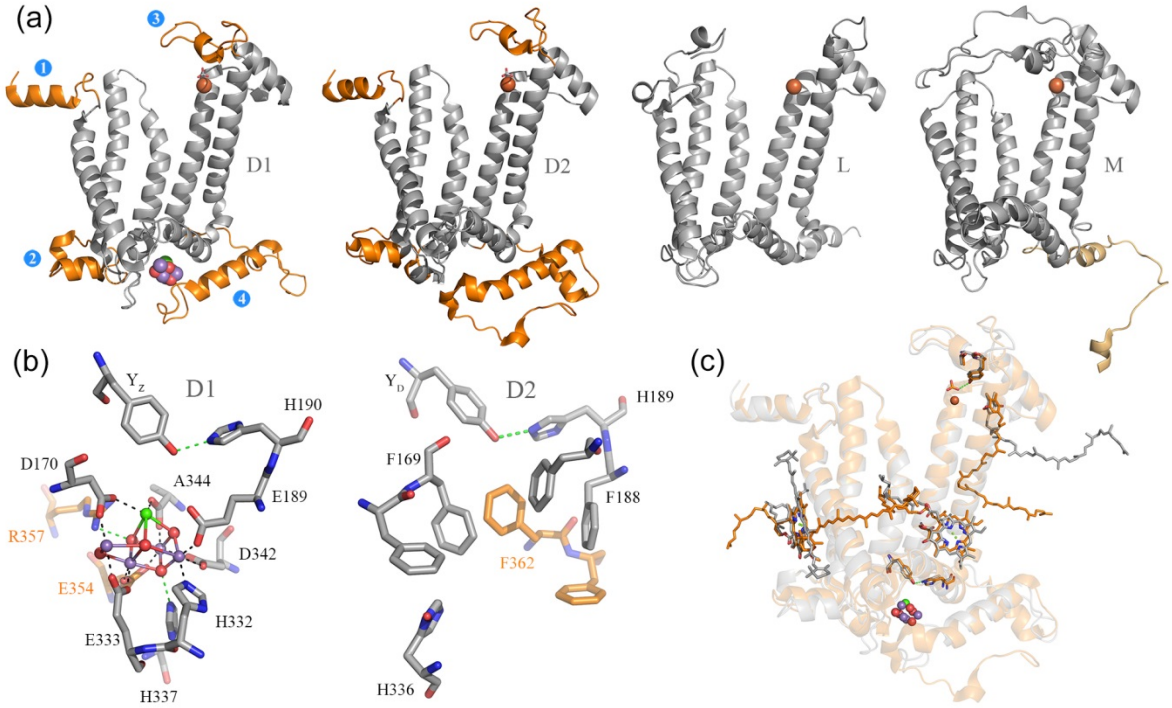
(a)
1
2
3
4
D1
D2
L
M
(b)
Y_Z
D1
H190
D170
A344
E189
R357
D342
E354
H332
E333
H337
Y_D
D2
H189
F169
F188
F362
H336
(c)

Fig. 2

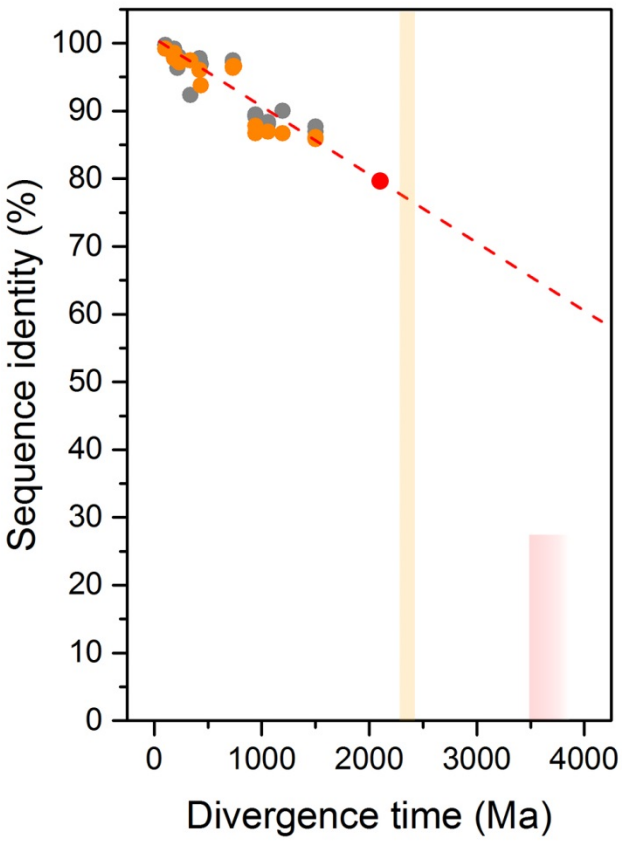
Sequence identity (%)
100
90
80
70
60
50
40
30
20
10
0
0
1000
2000
3000
4000
Divergence time (Ma)

Fig. 3

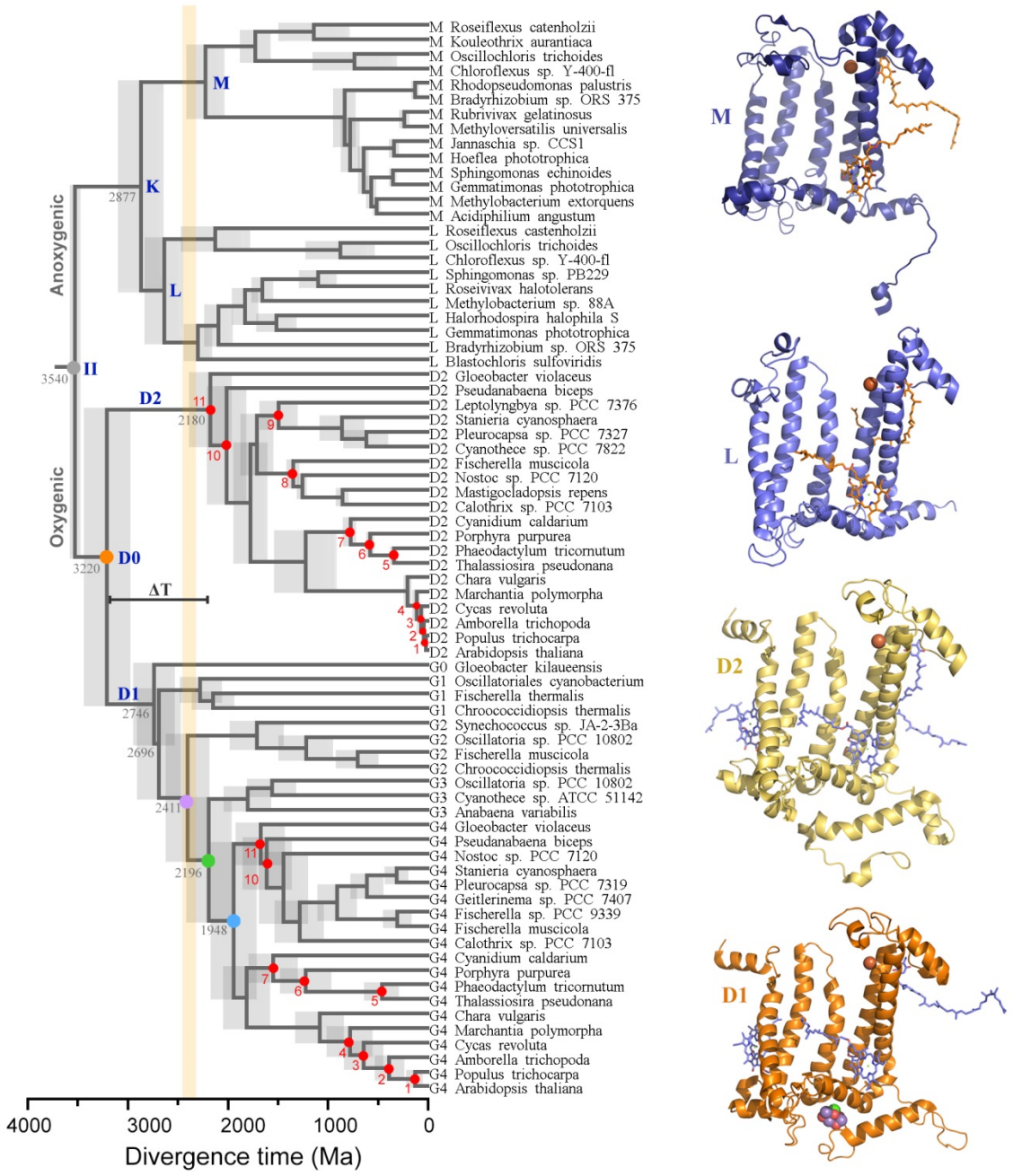
Anoxygenic
Oxygenic
M
K
L
II
D2
D0
D1
ΔT
2877
3540
2180
3220
2746
2696
2411
2196
1948
M Roseiflexus catenholzii
M Kouleothrix aurantiaca
M Oscillochloris trichoides
M Chloroflexus sp. Y-400-fl
M Rhodopseudomonas palustris
M Bradyrhizobium sp. ORS 375
M Rubrivivax gelatinosus
M Methyloversatilis universalis
M Jannaschia sp. CCS1
M Hoeflea phototrophica
M Sphingomonas echinoides
M Gemmatimonas phototrophica
M Methylobacterium extorquens
M Acidiphilium angustum
L Roseiflexus castenholzii
L Oscillochloris trichoides
L Chloroflexus sp. Y-400-fl
L Sphingomonas sp. PB229
L Roseivivax halotolerans
L Methylobacterium sp. 88A
L Halorhodospira halophila S
L Gemmatimonas phototrophica
L Bradyrhizobium sp. ORS 375
L Blastochloris sulfoviridis
D2 Gloeobacter violaceus
D2 Pseudanabaena biceps
D2 Leptolyngbya sp. PCC 7376
D2 Stanieria cyanosphaera
D2 Pleurocapsa sp. PCC 7327
D2 Cyanothece sp. PCC 7822
D2 Fischerella muscicola
D2 Nostoc sp. PCC 7120
D2 Mastigocladopsis repens
D2 Calothrix sp. PCC 7103
D2 Cyanidium caldarium
D2 Porphyra purpurea
D2 Phaeodactylum tricornutum
D2 Thalassiosira pseudonana
D2 Chara vulgaris
D2 Marchantia polymorpha
D2 Cycas revoluta
D2 Amborella trichopoda
D2 Populus trichocarpa
D2 Arabidopsis thaliana
G0 Gloeobacter kilaueensis
G1 Oscillatoriales cyanobacterium
G1 Fischerella thermalis
G1 Chroococcidiopsis thermalis
G2 Synechococcus sp. JA-2-3Ba
G2 Oscillatoria sp. PCC 10802
G2 Fischerella muscicola
G2 Chroococcidiopsis thermalis
G3 Oscillatoria sp. PCC 10802
G3 Cyanothece sp. ATCC 51142
G3 Anabaena variabilis
G4 Gloeobacter violaceus
G4 Pseudanabaena biceps
G4 Nostoc sp. PCC 7120
G4 Stanieria cyanosphaera
G4 Pleurocapsa sp. PCC 7319
G4 Geitlerinema sp. PCC 7407
G4 Fischerella sp. PCC 9339
G4 Fischerella muscicola
G4 Calothrix sp. PCC 7103
G4 Cyanidium caldarium
G4 Porphyra purpurea
G4 Phaeodactylum tricornutum
G4 Thalassiosira pseudonana
G4 Chara vulgaris
G4 Marchantia polymorpha
G4 Cycas revoluta
G4 Amborella trichopoda
G4 Populus trichocarpa
G4 Arabidopsis thaliana
4000
3000
2000
1000
0
Divergence time (Ma)
M
L
D2
D1

Fig. 4

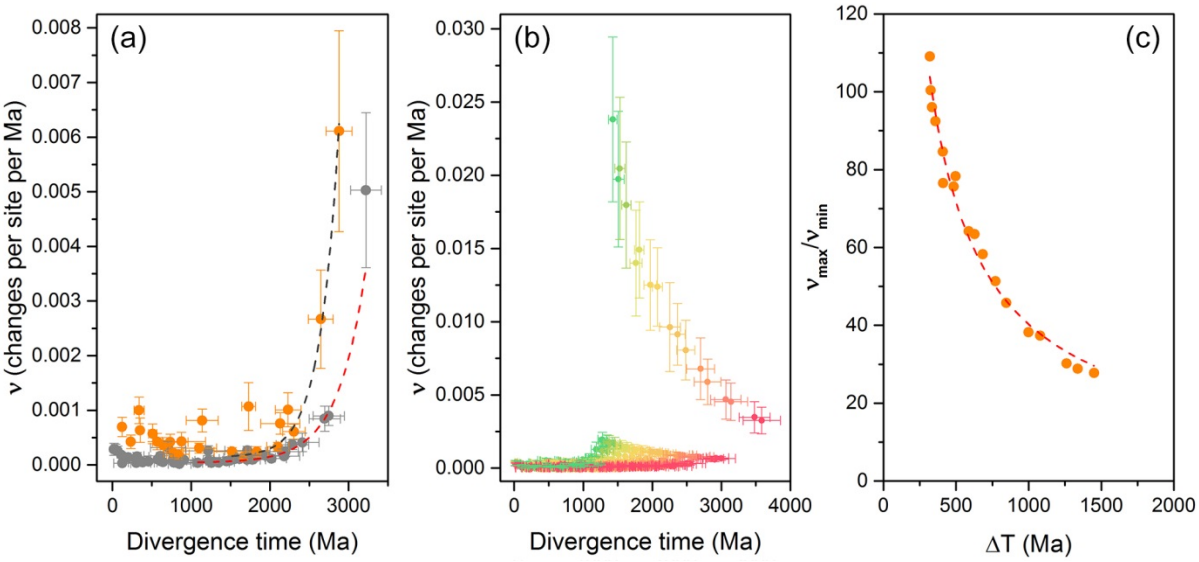
(a)
ν (changes per site per Ma)
Divergence time (Ma)
(b)
ν (changes per site per Ma)
Divergence time (Ma)
(c)
ν_{max}/ν_{min}
ΔT (Ma)

Fig. 5

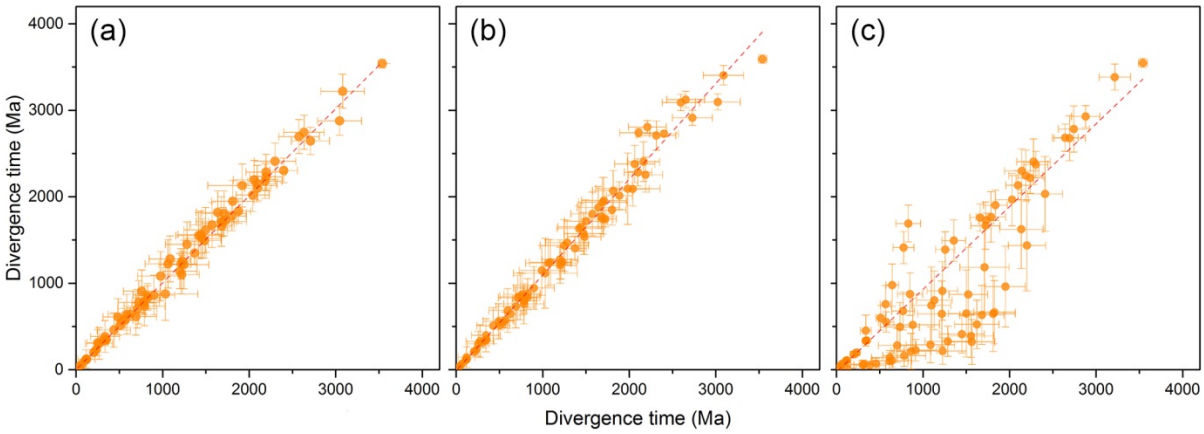
(a)
(b)
(c)
Divergence time (Ma)
Divergence time (Ma)
0
1000
2000
3000
4000

Fig. 6